Technology-driven methods for estimation of nature-based carbon stocks in Singapore

FINAL REPORT

FEBRUARY 2024

NUS National University of Singapore | Centre for Nature-based Climate Solutions
Faculty of Science

Supported by HSBC

Technology-driven methods for estimation of nature-based carbon stocks in Singapore

Final Report: February 2024

Prepared by: Khairun Nisha Binte Mohamed Ramdzan, Zu Dienle Tan, Leah Mary Lilly Denoun, H. Manjari Jayathilake, Annabel Jia Yi Lim, Yiwen Zeng, Hao Tang, and Lian Pin Koh

Centre for Nature-based Climate Solutions (CNCS),
Faculty of Science,
National University of Singapore

Funding Support: Hongkong and Shanghai Banking Corporation Limited, Singapore (HSBC)

Main Collaborators: Singapore Land Authority (SLA)
National Parks Board (NParks)

CONTENTS

ABBREVIATIONS, FIGURES AND TABLES

Abbreviations	
ACD	Aboveground carbon density
AGB	Aboveground biomass
BBNP	Bukit Batok Nature Park
BBTP	Bukit Batok Town Park
BTNR	Bukit Timah Nature Reserve
CCNR	Central Catchment Nature Reserve
DBH	Diameter at breast height
DI	Deionized
GLCM	Grey Level Co-occurrence Matrix
LiDAR	Light Detection and Ranging
LOOCV	Leave-one-out cross-validation
NbS	Nature-based solutions
RF	Random Forest
RMSE	Root-mean-squared error
SOC	Soil organic carbon
SD	Standard deviation
TOC	Total organic carbon
TNP	Thomson Nature Park
WNP	Windsor Nature Park

Tables	Page

EXECUTIVE SUMMARY

This report presents our findings on the development of spatially-explicit estimates of aboveground carbon in different forest ecosystem types and belowground carbon estimates across exotic-dominated secondary forest habitats in Singapore. The findings from this project pave the way for a cost-effective means of surveying and monitoring nature-based carbon projects, thereby ensuring the quality and credibility of the carbon credits they generate for nature-based solutions (NbS) for climate.

According to IUCN (2024), NbS for climate are efforts to protect, restore, and sustainably manage natural and modified ecosystems to increase carbon sequestration and reduce greenhouse gas emissions. The vast expanses of forests across the tropics represent many opportunities to implement NbS, such as carbon offset projects (hereafter referred to as 'carbon projects'). One of the factors that affects the potential to generate carbon credits or offset carbon emissions, is the forests' carbon sequestration potential. Developing effective, robust, and accurate methods for estimating the carbon stocks in various forest ecosystem types is therefore crucial for carbon projects.

Using Singapore as a testbed, this research project aims to develop a technology-driven method for estimating carbon across three forest ecosystem types, with an outlook for developing methodologies that can be scaled up across other forest areas in Southeast Asia. By using field measurements and remote sensing data (Light Detection and Ranging (LiDAR) data and satellite imageries), we develop ecosystem-specific models to predict aboveground carbon density (ACD) for Singapore's terrestrial forests, freshwater swamp forests, and mangroves. Ecosystem-specific models for this region are necessary to account for the spatial complexities and unique vegetation communities present in each forest ecosystem type, but which have not been adequately reflected in many carbon development projects. Equally not well reflected in carbon development projects is the belowground carbon stock. Hence, we also measure the belowground soil carbon for exotic-dominated secondary forests, which has limited information available in Singapore.

Key findings:

- Based on field measurements, freshwater swamp forests are the most carbon dense forest ecosystem in Singapore. All models predicted higher mean ACD for freshwater swamp forests (108.25 – 125.21 megagram of biomass carbon per hectare (Mg C ha^{-1}) compared to terrestrial forests (95.15 – 116.61 Mg C ha^{-1}) and mangroves (95.55 – 109.18 Mg C ha^{-1}). [Section 4.2 and 4.3]
- The forest ecosystems in Singapore store substantial amount of aboveground carbon. The models estimate 1.37 – 2.18 teragram of aboveground biomass carbon (Tg C) across the 14,930 ha of forests in Singapore in 2019. This equals to 2.74 – 4.35% of the 2021 national CO_2 emissions from fossil fuels. [Section 4.2 and 4.3]
- Our models partially explain the variation in ACD with the best performance for LiDAR-based models of freshwater swamp forests (R^2 = 0.64 – 0.74), followed by mangroves (R^2 = 0.54 – 0.60) and terrestrial forests (R^2 = 0.33 – 0.49). [Section 4.2]
- Exotic-dominated secondary forests play a role in carbon sequestration and contribute to belowground soil organic carbon (SOC) of 81.7 – 140.3 Mg C ha^{-1}. This was comparable to the SOC documented in other terrestrial forests in the non-swamp areas of Nee Soon (~167.9 Mg C ha^{-1}) and Bukit Timah Nature Reserve (~99.2 – 127.7 Mg C ha^{-1}) but was lesser than Nee Soon swamp (~528.1 Mg C ha^{-1}) and mangroves in Chek Jawa (~307.0 Mg C ha^{-1}). [Section 4.5]

1. INTRODUCTION

Nature-based climate solutions (NbS) can contribute to climate change mitigation by increasing carbon sequestration potential and reducing greenhouse gas emissions. It is estimated that the carbon mitigation potential of all NbS actions is 23.8 Pg CO_2e yr^{-1} (Griscom et al. 2017), a substantial portion of which can become financially viable projects (Koh et al. 2021). Aside from climate change mitigation, NbS can generate a slew of biodiversity and social co-benefits, such as water quality regulation and pollination (Sarira et al. 2022). As a result, NbS has been increasingly featured in countries' nationally determined contributions to nations' climate goals (Seddon et al. 2020).

There exists, however, concerns regarding the environmental integrity and credibility of NbS projects (Greenfield 2023). Challenges include providing additional carbon benefits compared to a business-as-usual scenario, ensuring long-term project permanence, preventing carbon-emitting activities from leakage (caused by carbon-emitting activities being displaced to nearby areas through project establishment), and enabling transparent and efficient monitoring and verification of carbon projects (Seymour & Langer 2021; Bode et al. 2015). It is, therefore, imperative that NbS deliver high-quality carbon that could address these challenges. To do so, robust, efficient, and accurate estimates of carbon stocks of forest ecosystems are needed.

Aboveground carbon stocks are primarily estimated using ground-based methods through field inventory measurements of trees. However, ground-based methods are limited in their spatial footprints (Zhao et al. 2018). Remote sensing technologies, such as light detection and ranging (LiDAR) technology and satellite imagery, allow the collection of surface data over larger spatial footprints of different vegetation species, over multiple timestamps, helping to scale up implementation and reduce labour/cost requirements of manual sampling (Asner & Mascaro 2014). As such, it is possible to develop ecosystem-specific models and spatially-explicit estimates of aboveground carbon density using a mixture of remote sensing technologies (Csillik et al. 2019).

In addition to the aboveground carbon stocks, the belowground soil carbon can be a major carbon pool contributing to climate change mitigation. In Singapore, secondary forests dominate the terrestrial forest ecosystem types, and the belowground carbon storage potential of native-dominated secondary forest (i.e. early succession and pioneer tree species) has been studied primarily in Central Catchment Nature Reserve (CCNR) and Bukit Timah Nature Reserve (BTNR) (Kleine et al. 2022; Chong et al. 2021; Ngo et al. 2013). However, belowground carbon storage in exotic-dominated secondary forest (i.e. plantation and agricultural tree species) has been largely understudied in Singapore (Kleine et al. 2022). By characterising and estimating both above- and belowground carbon, nuanced forest management strategies that potentially contribute to the nation's climate efforts could be developed.

This project, therefore, aims to develop aboveground carbon density (ACD) maps of three forest ecosystem types (terrestrial forest, freshwater swamp forest, and mangrove) in Singapore, and provide characterisations of belowground soil carbon for four exotic-dominated secondary forest sites. By developing aboveground carbon estimation models using field measurements and remote sensing technology across multiple forest ecosystem types in Singapore, the results of the project can produce extensive monitoring, reporting, and verification protocols for forest carbon estimates. Indeed, previous research estimating Singapore's forest carbon had focused mainly on ground-based methods limited to a few project sites (Lai et al. 2020; Neo et al. 2017; Friess et al. 2016; Ngo et al. 2013) or were not specific to any forest ecosystem types (NEA 2020). In addition to our work on ACD,

the belowground carbon estimates of exotic-dominated secondary forests provide a comprehensive assessment of the carbon pool in the Singapore's largest forest ecosystem type.

The main objectives of this project are to:

1. Develop LiDAR-Carbon models for different forest ecosystem types in Singapore using field measurements, allometric models, and LiDAR data.
2. Develop Satellite Imagery-LiDAR models using LiDAR-predicted aboveground carbon estimates with multispectral satellite imagery.
3. Generate aboveground carbon density maps for three main forest ecosystem types in Singapore.
4. Estimate belowground soil carbon for exotic-dominated secondary forests in Singapore.

2. STUDY SITES

Figure 1: A secondary forest area (Windsor Nature Park) in Singapore.

The study sites are categorised into the three most prominent forest ecosystem types in Singapore: terrestrial forests (primary and secondary vegetation), freshwater swamp forests, and mangroves. Based on the latest land use map in 2019 for Singapore, the areas of terrestrial forests, freshwater swamp forests, and mangroves cover are approximately 13,900 ha, 220 ha, and 810 ha respectively (Gaw et al. 2019).

2.1 Terrestrial forests (primary and secondary vegetation)

Primary forests are forests that are considered undisturbed. They are found in the Bukit Timah Nature Reserve (BTNR) and Central Catchment Nature Reserve (CCNR). These nature reserves are protected forests managed by the National Parks Board of Singapore (NParks) (Yee et al. 2019). The BTNR contains Singapore's largest remaining primary forest patch, extending over 164 ha, with an unlogged core forest area of about 48 ha (Ngo et al. 2016). The primary forest in BTNR is dominated by *Rubroshorea curtisii*, a hill dipterocarp forest tree species (Ngo et al. 2016, 2013). In comparison, the CCNR covers 1,662 ha and was originally mostly lowland dipterocarp forest; today, it consists mainly of secondary forest – albeit dominated by native tree species – with some areas of remnant dipterocarps that are considered primary forest in Singapore's context (Wong et al. 1994; Wang et al.

2022). The primary and secondary forests in the CCNR and BTNR cover approximately 2.49% of Singapore's total land area.

Secondary forests are defined as plant communities that have regrown on land that has been previously disturbed (i.e. cleared or cultivated) but in which a distinctly different structure and species composition from the primary forest have formed (Yee et al. 2016). In Singapore, secondary forests are classified into three types: i) native-dominated secondary forest/secondary regrowth forest (dominated by native tree species, i.e. parts of the CCNR and BTNR, Mandai, Southern Ridges), ii) exotic-dominated secondary forest from abandoned land (regrown from abandoned plantations or 'kampungs', i.e. Windsor forest, Bukit Batok Nature Park, Bukit Batok Town Park), and iii) waste woodlands (forests regrown on recently cleared land, after the 1960s) (Yee et al. 2016; Neo et al. 2017; Lai et al. 2020).

For this project, we collected field measurements for the following exotic-dominated secondary forest sites: Windsor Nature Park, Thomson Nature Park, Bukit Batok Nature Park, and Bukit Batok Town Park.

2.2. Freshwater swamp forest

The Nee Soon Freshwater Swamp Forest is located within the CCNR and is the last substantial tract of freshwater swamp forest left in Singapore (Cai et al. 2018; Chong et al. 2021). It covers approximately 100 ha and is a biologically-diverse habitat of high ecological significance and conservation value (Nguyen et al. 2022; Chong et al. 2021). The vegetation communities in Nee Soon are influenced by the soil and hydrology (Chong et al. 2021; Neo et al. 2017; Lai et al. 2021). As such, species characteristic of the freshwater swamp include *Baccaurea bracteata* (Phyllanthaceae)*, Lophopetalum multinervium* (Celastraceae), *Pandanus atrocarpus* (Pandanaceae), *Pometia pinnata* (Sapindaceae), and *Pternandra coerulescens* (Melastomataceae) (Nguyen et al. 2022; Chong et al. 2021).

2.3 Mangroves

Mangroves cover less than 1% of Singapore but are highly biodiverse (Yee et al., 2011). More than 30 mangrove vegetation genera, such as *Rhizophora*, *Avicennia, Bruguiera*, and *Lumnitzera* (Friess et al. 2016), can be found within the country. A large portion of these mangroves are located on offshore islands and the western and northern coasts of the main island, with the largest tract of mangroves located at Pulau Ubin (offshore) and Sungei Buloh Wetland Reserve (mainland) (Yang et al. 2012). The mangrove sites included in this report are Pasir Ris, Pulau Ubin, Mandai, Sungei Buloh, Kranji, and Lim Chu Kang (Friess et al. 2016; Phang et al. 2015; Shribman et al. 2024, 2023).

3. RESEARCH METHODOLOGY

3.1 Summary

The methodology consists of three main steps (Fig. 2): A) field measurements to estimate aboveground biomass (AGB) and aboveground carbon density (ACD), and B) the development of ecosystem-specific Light Detection and Ranging (LiDAR)-Carbon models and C) Satellite Imagery-LiDAR models to estimate LiDAR-predicted ACD and Satellite-predicted ACD of the terrestrial forests, freshwater swamp forests, and mangroves in Singapore. These methods were applied to both 2014 and 2019 datasets.

Firstly, the AGB and ACD of all study sites were calculated from field inventory measurements provided by collaborators or collected by our team (Fig. 2 Box A). Next, a two-step modelling approach composed of machine learning technique was applied for each forest ecosystem type to first relate field-measured ACD to LiDAR metrics to develop the LiDAR-Carbon models (Fig. 2 Box B), then incorporate satellite-derived metrics to the LiDAR-predicted ACD to develop the Satellite Imagery-LiDAR models (Fig. 2 Box C).

The LiDAR metrics used in these models were obtained from Singapore Land Authority (SLA) for 2014 and 2019, and processed for height- and canopy-related metrics at a 1 x 1 m resolution. The satellite-derived metrics were obtained from online sources of optical and radar satellite datasets (i.e. Landsat and PALSAR) for all years of field measurements, and were extracted for vegetation indices and texture properties at 30 x 30 m resolution. The two-step modelling approach was chosen to preserve the high-resolution LiDAR data which provide three-dimensional forest structure for accurate ACD predictions, while the satellite-derived metrics provide the forest conditions during field measurements that were not captured in the LiDAR 2014 and 2019 datasets. Furthermore, as wall-to-wall LiDAR data is costly, establishing the relationships in the second predictive model using readily available satellite data allows for spatial and temporal extrapolation of aboveground carbon.

In addition to our work on ACD, we collected soil cores from exotic-dominated secondary forest to measure belowground soil carbon because it has been largely understudied even though it is the predominant type of terrestrial secondary forest ecosystem in Singapore (Kleine et al. 2022; Yee et al. 2019).

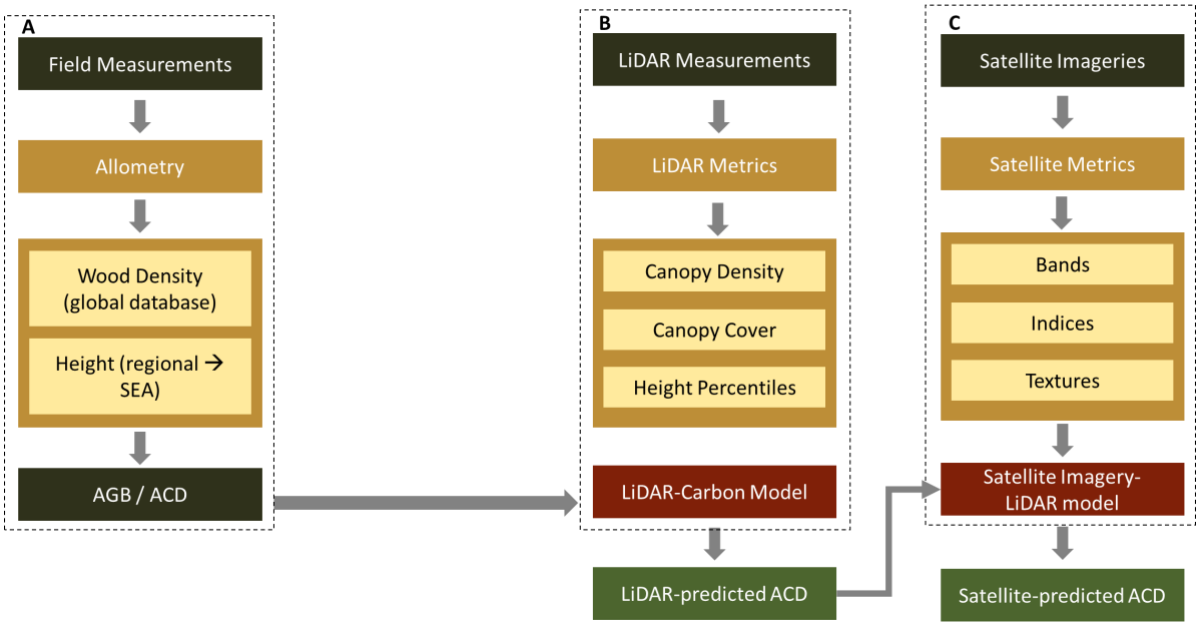

Figure 2: Overview of the workflow for developing the LiDAR-Carbon and Satellite Imagery-LiDAR models.

3.2 Field inventory measurements (Fig. 2 Box A)

Field inventory measurements of the forests were obtained from collaborators and/or available literature (Table 1). Briefly, 20 x 20 m (0.04 ha) square plots were established within all terrestrial and freshwater swamp forest sites. The diameter at breast height (DBH) of trees greater than 5 cm was taken at a standard height of 1.3 m (Ngo et al. 2013; Chong et al. 2021). Each tree was also identified to the species level to obtain the species-specific wood density extracted from a global database. The majority of the terrestrial forests were sampled twice, once in 2012 – 2013 (Fig. 3a) and a second time in 2018 – 2023 (Fig. 3b). The only exception was the 'novel forest' (i.e. recovering forest post-land abandonment) and the Central Catchment Nature Reserve (CCNR), which were only surveyed once in 2011 and 2022, respectively (Fig. 3) (Neo et al. 2017; Er et al., 2023).

Additional field inventory measurements were collected for this project to support NParks' Long-Term Forest Ecological Monitoring project (Er et al. 2023). Fieldwork was conducted from June – August 2023, following a sampling protocol similar to the one described above for collection of forest measurements from the secondary forests in Bukit Batok Town Park, Bukit Batok Nature Park, Windsor Nature Park, and Thomson Nature Park (Fig. 3a).

For mangroves, the plots used in this project were selected to represent different geomorphological settings, which influence the mangroves' carbon stocks and fluxes (Friess et al. 2016). Tree measurements for the various mangrove sites were collected from established circular plots with a 7 m radius, measured in two time periods: 2014 and 2022 – 2023 (Fig. 3).

Table 1: Summary of the field measurement plots at the study sites.

Field collection period (Year)	Forest ecosystem type	Sites	Number of plots	Plot size (ha)	Plot dimensions	Source of field measurement data
Included in 2019 models						
2018	Terrestrial (Secondary) forest	Non-swamp areas of Nee Soon	19	0.04	20 x 20 m	(Chong et al. 2021)
2019	Terrestrial (Primary) forest	Bukit Timah Nature Reserve (BTNR)	50	0.04	20 x 20 m	(Ngo et al. 2013)
2019	Terrestrial (Secondary) forest	Bukit Timah Nature Reserve (BTNR)	50	0.04	20 x 20 m	
2022	Terrestrial (Primary and secondary) forests	Central Catchment Nature Reserve (CCNR)	57	0.04	20 x 20 m	NParks
2023	Terrestrial (Secondary) forest	Bukit Batok Town Park (BBTP)	5	0.04	20 x 20 m	NUS CNCS and NParks
2023	Terrestrial (Secondary) forest	Thomson Nature Park (TNP)	5	0.04	20 x 20 m	
2023	Terrestrial (Secondary) forest	Bukit Batok Nature Park (BBNP)	5	0.04	20 x 20 m	
2023	Terrestrial (Secondary) forest	Windsor Nature Park (WNP)	5	0.04	20 x 20 m	
2018	Freshwater swamp forest	Nee Soon Freshwater Swamp Forest	21	0.04	20 x 20 m	(Chong et al. 2021)
2022	Freshwater swamp forest	Central Catchment Nature Reserve (CCNR)	3	0.04	20 x 20 m	NParks
2022/2023	Mangrove	Lim Chu Kang, Sungei Buloh, Mandai, Pasir Ris, Sungei Ubin, Sungei Puaka, Sungei Jelutong, Chek Jawa, Pandan, Pulau Semakau, Berlayer Creek	51	0.015	7 m radius (circular)	(Shribman et al. 2024, 2023)
Included in 2014 models						
2011	Terrestrial (Secondary) forest	Novel forest: Tampines North, Tampines Ave 10, Tampines Ave 1, Lentor, Clementi	77	0.04	20 x 20 m	(Neo et al. 2017)

		forest, Dover forest, Greenleaf forest, Ulu Pandan bus depot, Bukit Batok Hillside Park, Kranji woodland, Senja woods, Admiralty park				
2012	Terrestrial (Primary) forest	Bukit Timah Nature Reserve (BTNR)	50	0.04	20 x 20 m	(Ngo et al. 2013)
2012	Terrestrial (Secondary) forest	Bukit Timah Nature Reserve (BTNR)	50	0.04	20 x 20 m	
2013	Terrestrial (Secondary) forest	Non-swamp areas of Nee Soon	19	0.04	20 x 20 m	(Chong et al. 2021)
2013	Terrestrial (Secondary) forest	Bukit Batok Town Park (BBTP)	5	0.04	20 x 20 m	(Neo et al. 2017)
2013	Terrestrial (Secondary) forest	Thomson Nature Park (TNP)	5	0.04	20 x 20 m	
2013	Terrestrial (Secondary) forest	Bukit Batok Nature Park (BBNP)	5	0.04	20 x 20 m	
2013	Terrestrial (Secondary) forest	Windsor Nature Park (WNP)	5	0.04	20 x 20 m	
2013	Freshwater swamp forest	Nee Soon Freshwater Swamp Forest	21	0.04	20 x 20 m	(Chong et al. 2021)
2014	Mangrove	Pasir Ris, Chek Jawa, Mandai, Sungei Buloh	40	0.015	7 m radius (circular)	(Friess et al. 2016; Phang et al. 2015)

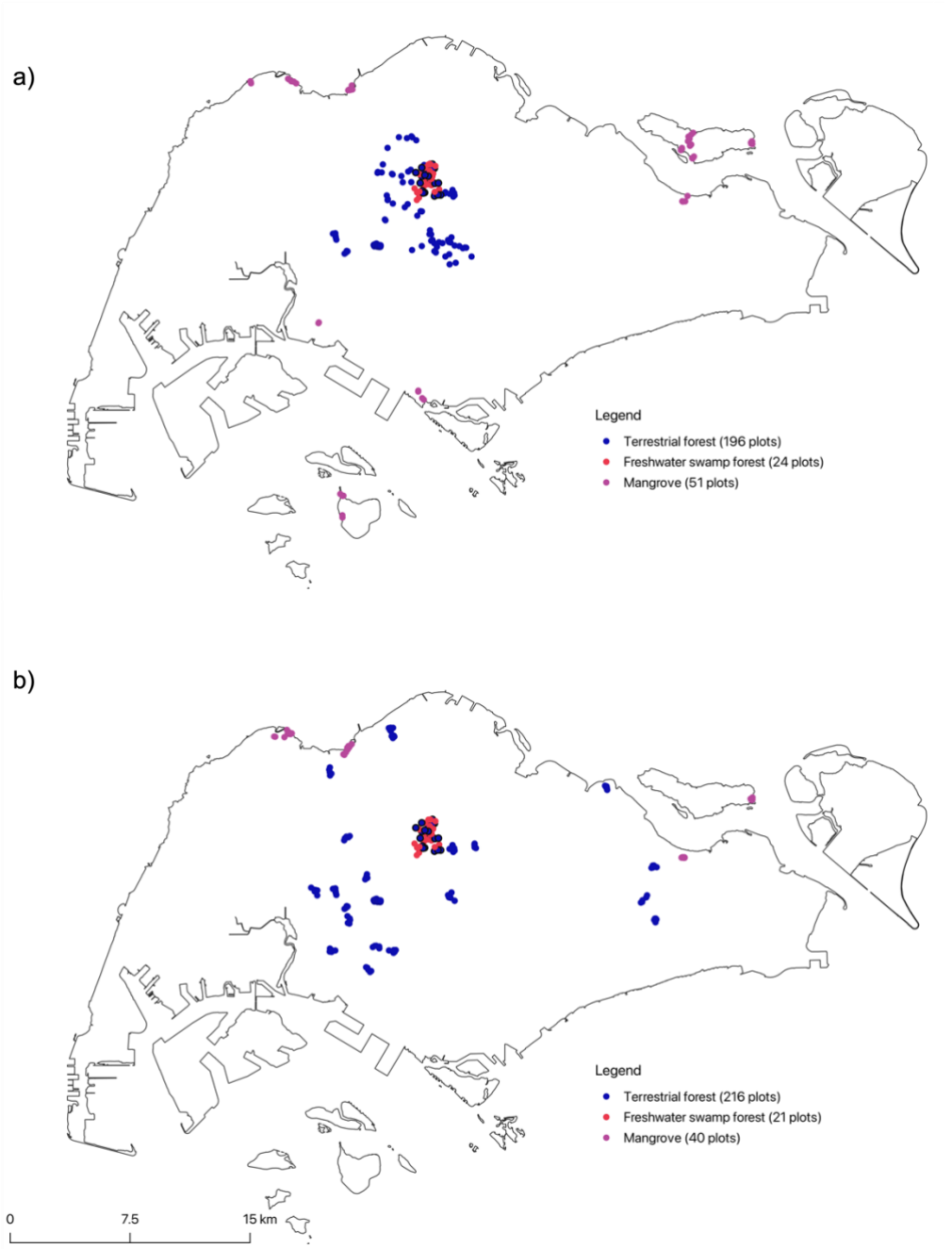

Figure 3: Locations of the terrestrial forests, freshwater swamp forest, and mangroves study sites for (a) 2018 – 2023, and (b) 2011 and 2014.

3.2.1 Converting field measurements to aboveground biomass and carbon estimates

A general pantropical allometric model was used to calculate the field-measured plot-level AGB (Chave et al. 2014) (Eq. 1):

$$AGB = 0.0673(D^2 H\rho)^{0.976} \quad [1]$$

Where D = DBH (cm), H = tree height (m), and ρ = species-specific wood density (g cm^{-3}). The resultant AGB values were then multiplied by 0.475 to obtain field-measured ACD values (IPCC 2006).

As tree height can be underestimated due to dense canopy cover for some study sites, we estimated height using the height-DBH models in the *BIOMASS* package (Réjou-Méchain et al. 2017). The *BIOMASS* package features four models: Michaelis-Menten, Weibull, and two log functions (Box 1). We fitted all models using the DBH of the trees in the Tallo global tree allometry and crown architecture database (Jucker et al. 2022) for the tree genus found in our study sites. We then compared the modelled height to the existing height values within the database to determine the best model. For most of the tree genus in each forest ecosystem type, the Weibull function showed the best performance (Table A1) and was therefore used to predict the height of all trees in each forest ecosystem type.

Species-specific wood density data for each tree were obtained from the Global Wood Density Database (Chave et al. 2009). For species not listed in the database, genus-averaged wood density values were used instead.

All field-measured ACD were subsequently included in either the 2019 or 2014 models (Table 1).

Box 1 **Height-DBH models**

Log 1: $log(H) = \boldsymbol{a} + \boldsymbol{b} * log(D)$

Log2: $log(H) = \boldsymbol{a} + \boldsymbol{b} * log(D) + \boldsymbol{c} * log(D)^2$

Weibull: $H = \boldsymbol{a} * \left(1 - exp(-(D/\boldsymbol{b})^{c})\right)$

Michaelis: $H = (\boldsymbol{a} * D)/(\boldsymbol{b} + D)$

D = Tree diameter (cm)

H = Tree height (m)

a = Intercept of the model

b = Model estimate

c = Model estimate

3.3 Developing ecosystem-specific LiDAR-Carbon models (Fig. 2 Box B)

LiDAR data covering the entire island of Singapore and some of the offshore islands were obtained from the Singapore Land Authority (SLA). The LiDAR footprints were collected over two temporal periods, 2014 and 2019. The data was collected using an airborne, long-range LiDAR scanning system with integrated Global Positioning System-Inertial Measurement Unit to produce 3D point cloud data with an average point density of 12.90 points per m^2. The point clouds were processed and classified using LAStools (Isenburg 2014) and QGIS (QGIS.org) to extract 21 LiDAR height- and canopy- metrics at a 1 x 1 m resolution (Table A2). The LiDAR metrics were further categorized into different forest ecosystem types using a vegetation landcover map (Gaw et al. 2019) (Table 2).

Table 2: The types of vegetation layers and corresponding ecosystem types.

No	Vegetation layers	Forest ecosystem type	Considered for the ACD estimates models?
1	Vegetation with limited human management (with tree canopy)	Terrestrial forest	Yes
2	Vegetation with limited human management (without tree canopy)	N/A	No
3	Vegetation with structure dominated by human management (with tree canopy)	Trees-outside-forest	No
4	Vegetation with structure dominated by human management (without tree canopy)	N/A	No
5	Freshwater swamp forest	Fresh water swamp forest	Yes
6	Freshwater marsh	N/A	No
7	Mangrove forest	Mangrove	Yes

We constructed 2014 and 2019 LiDAR-Carbon models for different ecosystem types using field-measured ACD and the LiDAR metrics (Asner & Mascaro 2014). The data for each forest ecosystem type was split into 75% training and 25% testing datasets using a stratified random strategy from three percentile groups in the *caret* package (Kuhn et al. 2016). We considered all LiDAR metrics to be independent variables and the field-measured ACD to be the dependent variable.

We used the Random Forest (RF) algorithm (Breiman 2001) to develop the models on the training datasets. This is a general-purpose machine learning technique that utilises decision trees to approximate relationships between variables (Zhao et al. 2018). Further, it is a recursive ensemble method that can reduce the effects of the underdispersion (Wang et al. 2023) and is robust to outliers. We used the *caret* package (Kuhn et al. 2016) in the R statistical language (R Core Team 2022) to develop and tune our LiDAR-Carbon models. We additionally performed repeated cross-validation to evaluate the performance of our models on the training dataset. To test the accuracy of each LiDAR-Carbon model, we regressed the ACD from the testing dataset against the predicted ACD. Finally, we used the models to predict ACD across each forest ecosystem type.

3.4 Developing ecosystem-specific Satellite Imagery-LiDAR models (Fig. 2 Box C)

A combination of optical and radar data was used to develop the Satellite Imagery-LiDAR models (Table 3) (Urbazaev et al. 2018). Multi-year nationwide optical composites from Landsat 8 OLI/TIRS (available online: https://www.usgs.gov/landsat-missions) at 30 x 30 m resolution were downloaded using Google Earth Engine code developed by De Alban et al. (2018). Five-year composites were chosen to cover the length of time when the field measurements were collected (Table 3). Five indices

related to vegetation health and productivity were calculated, including the Normalized Difference Vegetation Index (NDVI), the Enhanced Vegetation Index (EVI), the Soil-Adjusted Total Vegetation Index (SATVI), the Normalized Difference Tillage Index (NDTI), and the Land Surface Water Index (LSWI) (De Alban et al. 2018). In addition to the bands and indices, we also extracted the Gray Level Co-occurrence Matrix (GLCM) textures for classifying vegetation (De Alban et al. 2018; Haralick et al. 1973).

For the radar data, we used the Advanced Land Observing Satellite Phased Array type L-band Synthetic Aperture Radar (ALOS-2/PALSAR-2) (Table 3) at 30 x 30 m resolution (available online: https://www.eorc.jaxa.jp/ALOS/en/index_e.htm). Two polarizations are available for PALSAR data: Horizontal transmit-horizontal receive (HH) and horizontal transmit-vertical receive (HV) (Yommy et al. 2015). Multiple indices and textures were extracted from the radar data. The former included indices extracted from the two polarization channels: HH/HV, HV/HH, average of the polarizations (AVE), difference between HH and HV (DIF), normalized difference index (NDI), and the Normalized L index (NLI). Extracted textures included the contrast (CON), dissimilarity (DIS), inverse difference moment (IDM), angular second moment (ASM), entropy (ENT), mean (AVG), correlation (COR), and variance (VAR) textures (De Alban et al. 2018; Haralick et al. 1973). All images were imported and pre-processed using Google Earth Engine public catalogue (Gorelick et al. 2017).

Table 3. Satellite metrics and data collection time period for the Satellite Imagery-LiDAR models.

	Landsat 8 OLI/TIRS	ALOS-2/PALSAR-2
Data collection time period (2014 Model)	2011 – 2015	2015
Data collection time period (2019 Model)	2018 – 2022	2019
Metrics	7 bands 5 indices 240 GLCM textures	HH, HV polarizations 4 indices 80 GLCM textures

Similarly to the LiDAR-Carbon models, we built the Satellite Imagery-LiDAR models for 2014 and 2019 using a RF approach. The independent variables were the satellite bands, indices, and Grey Level Co-occurrence Matrix (GLCM) textures, whereas the dependent variable was the LiDAR-predicted ACD. All variables used in the models were resampled to 100 x 100 m resolution due to long processing time for higher resolution analysis. Similar model selection, finetuning, and performance evaluation as the LiDAR-Carbon models were conducted for the Satellite Imagery-LiDAR models (Probst et al. 2019). Finally, we used the models to predict ACD across different forest ecosystem types.

3.5 Comparisons between field-measured ACD and predicted ACD

To determine whether the models were able to accurately predict ACD of the study sites, we compared the LiDAR-predicted and Satellite-predicted ACD to its respective field-measured ACD. These comparisons between the predicted and field-measured ACD in each forest ecosystem type acts as a verification to test the performance of the models. Using a Tukey's (post-hoc) statistical test, we determine whether the field-measured ACD and predicted ACD for all study sites were significantly

different. The difference was calculated between the mean of each measured or predicted ACD dataset, and the mean of all ACD datasets, for each forest ecosystem type and year. The significance of this difference was determined using 95% confidence intervals in the 'multcompView' package (Graves et al. 2023).

3.6 Field-measured estimation of belowground soil carbon

In addition to our work on ACD, we calculated belowground soil carbon for exotic-dominated secondary forest in Singapore, which is the predominant type of terrestrial secondary forest ecosystem in Singapore (Kleine et al. 2022; Chong et al. 2021; Ngo et al. 2013). As the belowground soil carbon of exotic-dominated secondary forest (i.e. plantation and agricultural tree species) has been largely understudied (Kleine et al. 2022), the main study sites were located in these forest ecosystems at Bukit Batok Town Park, Bukit Batok Nature Park, Windsor Nature Park, and Thomson Nature. Soil cores were taken at the centre of the plots in these forest sites from June – August 2023 to estimate belowground carbon (Fig. 4).

A regular soil auger was used to collect soil samples up to a maximum depth of two meters, depending on the difficulty of retrieving the soil cores (Fig. 4). Three soil cores were taken from the vegetation plots for each site, except for Windsor Nature Park, which had four soil cores. The soil cores were subsampled at every 10 cm depth in the field.

Three parameters were required to calculate belowground soil carbon: the dry bulk density, total organic carbon content, and the soil depth interval. The bulk density was calculated by dividing the mass of the dried soil sample by the known volume of the wet soil sample (Kauffman & Donato 2012) (Eq. 3):

$$Dry\ bulk\ density\ (g\ cm^{-3}) = \frac{Oven\ dry\ sample\ mass\ (g)}{Soil\ sample\ Volume\ (m^3)} \quad [2]$$

The dried soil for each sample was then grounded into fine powder. An equal amount of grounded soil samples (30 mg) from each soil depth interval (0-10 cm, 10-30 cm, 30-50 cm, 50-100 cm, 100-150 cm, and 150-200 cm) was acid fumigated (Harris et al. 2001) and dried before being used for total organic carbon (TOC) analysis. The TOC (%) of the soil samples were determined by the Elementar Vario TOC analyser (Harris et al. 2001). The soil organic carbon (SOC) at each depth interval was then calculated using the following equation (Kauffman & Donato 2012) (Eq. 4):

$$Belowground\ organic\ soil\ carbon\ (Mg\ C\ ha^{-1}) = Dry\ bulk\ density\ (g\ cm^{-3}) \times Soil\ depth\ interval\ (cm) \times\ TOC\ (\%) \quad [3]$$

The total sum and mean of SOC for up to 100 cm, 150 cm, and 200 cm were calculated for each soil core (Kauffman & Donato 2012; Ngo et al. 2013).

Figure 4: Soil samples were collected at every 10 cm depth intervals using a normal auger head down to 150 – 200 cm depth.

4. RESULTS

4.1 Field-measured ACD

The mean field-measured ACD was the highest for freshwater swamp forests at 120.20 – 120.30 Mg C ha^{-1} followed by terrestrial forests (113.34 – 116.87 Mg C ha^{-1}) and mangroves (108.88 – 118.12 Mg C ha^{-1}) (Table 4). However, the largest range of ACD in 2019 was observed in terrestrial forests (7.78 – 789.30 Mg C ha^{-1}), followed by freshwater swamp forests (32.64 – 509.95 Mg C ha^{-1}), and mangroves (7.14 – 336.45 Mg C ha^{-1}) (Table 4; Fig. 5).

Table 4. Summary statistics of field-measured ACD by forest ecosystem type for 2019 and 2014.

	Forest ecosystem type	Mean ACD (Mg C ha^{-1})	Standard error (Mg C ha^{-1})	Minimum – Maximum ACD (Mg C ha^{-1})
2019				
1	Terrestrial forests (primary and secondary) (n = 196)	116.87	6.52	7.78 – 789.30
2	Freshwater swamp forests (n = 24)	120.30	19.92	32.64 – 509.95
3	Mangroves (n = 51)	108.88	8.89	7.14 – 336.45
2014				
1	Terrestrial forests (primary and secondary) (n = 216)	113.34	7.25	9.33 – 739.44
2	Freshwater swamp forests (n = 21)	120.20	23.95	33.29– 531.83
3	Mangroves (n = 40)	118.12	11.79	25.14 – 342.63

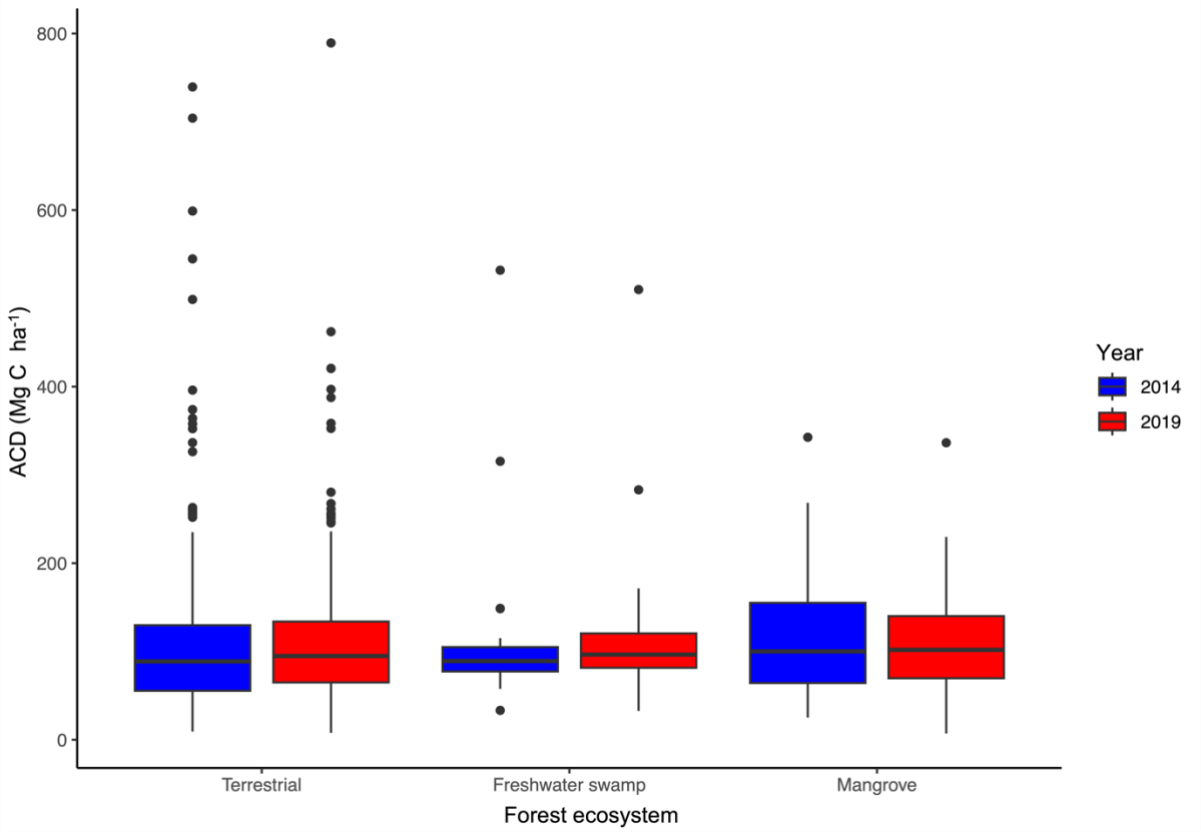

Figure 5: Boxplots showing variations in field-measured ACD in the three forest ecosystem types for 2014 and 2019.

4.2 Ecosystem-specific LiDAR-Carbon models and LiDAR-predicted ACD

A LiDAR-Carbon model was developed for each forest ecosystem type in 2014 and 2019 using the training datasets and a random forest (RF) approach. However, for clarity, we present the results from 2014 and 2019 together in the following sections. The ranked importance of the independent variables for each model differed between the forest ecosystem types and the model year (Fig. A1). In general, the various canopy height percentiles were important in explaining the ACD for all models, while the relative height density had lower importance.

The LiDAR-Carbon models' performance (R^2) for all forest ecosystem types was the best for freshwater swamp forests (R^2 = 0.64 – 0.74; RMSE = 62.46 – 69.54 Mg C ha^{-1}), followed by mangroves (R^2 = 0.54 – 0.60; RMSE = 44.62 – 69.96 Mg C ha^{-1}) and terrestrial forests (R^2 = 0.33 – 0.49; RMSE = 78.45 – 80.99 Mg C ha^{-1}) (Table 5). However, it is important to note that the small training data sample size (n = ~17 – 18) used in the models for freshwater swamp forests could have overfitted the relationships. The performance of these models on the testing datasets ranged from R^2 = 0.15 – 0.45 for all forest ecosystem types (Table 5 and Fig. A2).

Table 5: Performance of the ecosystem-specific LiDAR-Carbon models. The standard deviation (SD) of the R-squared and RMSE values for the cross-validation of the LiDAR-Carbon training models is reported. The number of samples in the models is represented by the n-values (n = training dataset: testing dataset).

		Training		Testing	
	Forest ecosystem type (Training: testing datasets)	**Mean R^2 ± SD R^2**	**RMSE ± SD Mg C ha^{-1}**	**R^2**	**RMSE (Mg C ha^{-1})**
2019					
1	Terrestrial forests (primary and secondary) (n = 148:48)	0.33 ± 0.26	78.45 ± 32.35	0.33	66.61
2	Freshwater swamp forests (n = 18:6)	0.64 ± 0.33	69.54 ± 64.79	0.31	71.51
3	Mangroves (n = 39:12)	0.54 ± 0.33	44.62 ± 17.56	0.45	67.39
2014					
1	Terrestrial forests (primary and secondary) (n = 162:54)	0.49 ± 0.22	80.99 ± 30.60	0.34	62.41
2	Freshwater swamp forests (n = 17:4)	0.74 ± 0.35	62.46 ± 65.70	0.16	42.30
3	Mangroves (n = 30:10)	0.60 ± 0.38	69.96 ± 32.59	0.15	69.88

Two maps of the predicted ACD in 2014 and 2019 were generated from the LiDAR-Carbon models (Fig. 6; hereafter referred to as "LiDAR-predicted ACD"). The mean LiDAR-predicted ACD in Singapore for 2019 was the highest for terrestrial forests (116.61 Mg C ha^{-1}), followed by freshwater swamp forests (112.41 Mg C ha^{-1}) and mangroves (97.90 Mg C ha^{-1}) (Table 6). However, different trends were observed in 2014 with the highest mean LiDAR-predicted ACD found in freshwater swamp forests (125.21 Mg C ha^{-1}) followed by mangroves (108.72 Mg C ha^{-1}) and terrestrial forests (98.13 Mg C ha^{-1}) (Table 6). The difference in trends could be due to the different sampling sites with different forest conditions for the field measurements used to develop the 2014 and 2019 terrestrial forests models. This resulted in the larger range in LiDAR-predicted ACD for terrestrial forest ecosystems in 2014 (21.22 – 631.11 Mg C ha^{-1}) and 2019 (46.63 – 499.78 Mg C ha^{-1}) (Table 6). Despite these difference, the terrestrial forests models showed consistent high ACD for Bukit Timah Nature Reserve and Central Catchment Nature Reserve with 120.44 – 147.88 Mg C ha^{-1} for 2019 and 117.40 – 166.28 Mg C ha^{-1} for 2014.

The spatial distribution of the LiDAR-predicted ACD in 2014 and 2019 was similar for all forest ecosystem types (Fig. 6). Areas with high predicted ACD (>100 Mg C ha^{-1}) were concentrated in the Central Catchment Nature Reserve, Nee Soon Swamp Forest, Bukit Timah Nature Reserve, MacRitchie Reservoir Park, Coney Island, Sungei Buloh Wetland Reserve, and the eastern end of Pulau Ubin (near Chek Jawa). Areas with low predicted ACD (<100 Mg C ha^{-1}) were concentrated in the forest around Western Water Catchment, the northern part of Tengah airbase, Poyan reservoir, and parts of Pulau Ubin (near Sungei Jelutong and Ubin quarry).

Overall, the total predicted ACD from the LiDAR-Carbon models in 2019 for terrestrial forests, freshwater swamp forests, and mangroves were 1.28 Tg C, 0.02 Tg C, and 0.07 Tg C respectively. The total predicted ACD in 2019 for all forest ecosystem types is 1.37 Tg C, equivalent to 2.74% of the totally national emissions of carbon dioxide from fossil fuels in 2021, which is estimated to be 50.09 Tg CO_2 (NEA 2021).

Table 6: Summary statistics of the LiDAR-predicted ACD and the standard deviation (SD) for the different forest ecosystem type for 2014 and 2019.

	Forest ecosystem type	Mean ± SD ACD (Mg C ha^{-1})	Minimum – Maximum ACD (Mg C ha^{-1})
2019			
1	Terrestrial forests (primary and secondary)	116.61 ± 60.37	46.63 – 499.78
2	Freshwater swamp forests	112.41 ± 59.63	59.57 – 357.07
3	Mangroves	97.90 ± 44.33	31.09 – 181.94
2014			
1	Terrestrial forests (primary and secondary)	98.13 ± 72.93	21.22 – 631.11
2	Freshwater swamp forests	125.21 ± 56.59	56.86 – 359.95
3	Mangroves	108.72 ± 22.95	73.17 – 178.25

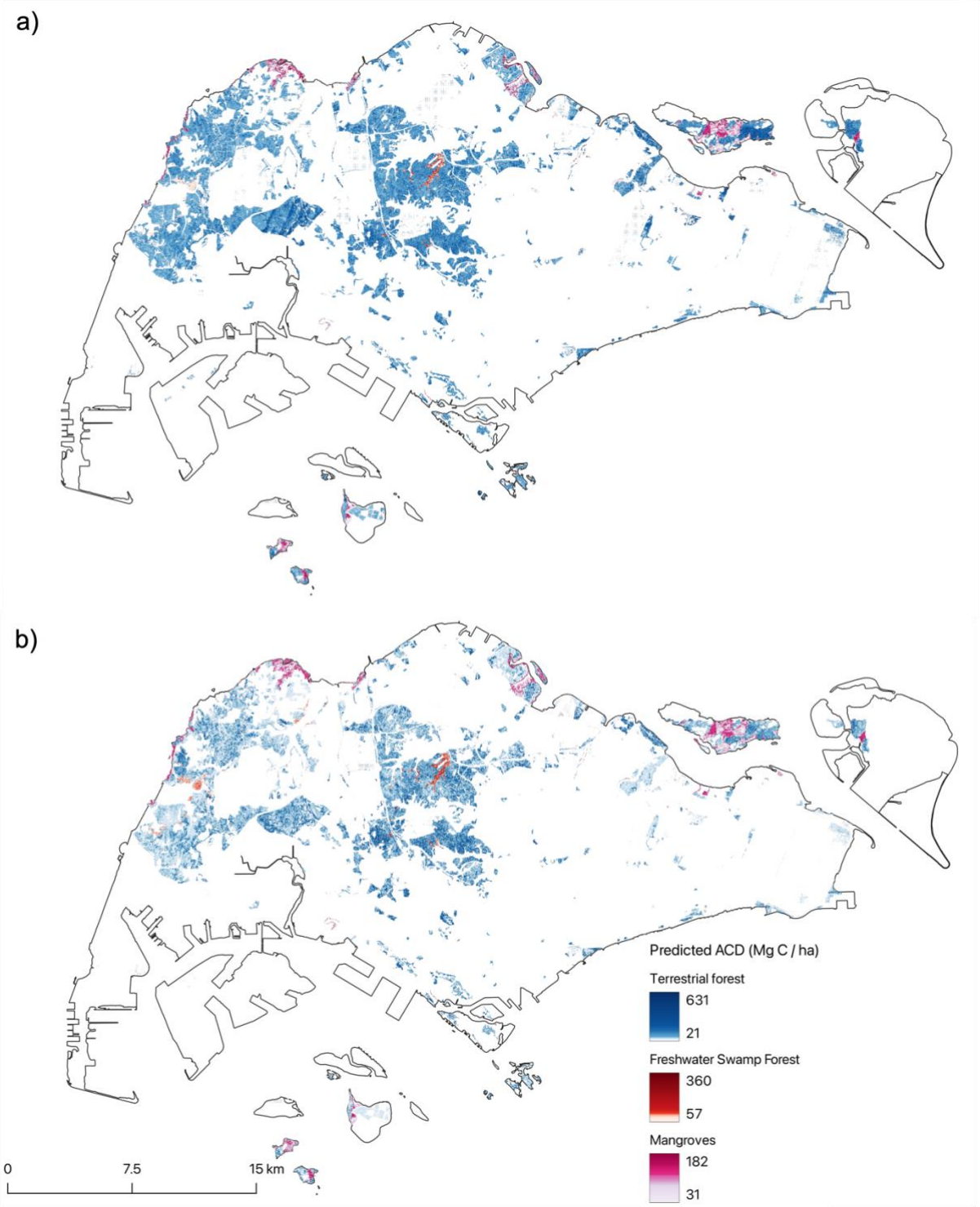

Figure 6: LiDAR-predicted ACD for a) 2019 and b) 2014 by forest ecosystem type.

4.3 Ecosystem-specific Satellite Imagery-LiDAR models and Satellite-predicted ACD

A Satellite Imagery-LiDAR model was developed for each forest ecosystem type in 2014 and 2019. The ranked importance of the satellite metrics differed between the forest ecosystem type and model year (Fig. A3). Overall, optical satellite metrics were ranked by the models as more important in explaining the LiDAR-predicted ACD compared to radar metrics (Fig. A3).

The Satellite Imagery-LiDAR models' performance (R^2) for all forest ecosystem types was the best for freshwater swamp forests (R^2 = 0.38 – 0.41; RMSE = 28.30 – 30.85 Mg C ha^{-1}), followed by mangroves (R^2 = 0.38 – 0.43; RMSE = 12.02 – 21.43 Mg C ha^{-1}) and terrestrial forests (R^2 = 0.23 – 0.29; RMSE = 36.81 – 37.92 Mg C ha^{-1}) (Table 7). The performance of these models on the testing datasets ranged from R^2 = 0.26 – 0.44 for all forest ecosystem types (Table 7 and Fig. A4).

Table 7: Performance of the ecosystem-specific Satellite Imagery-LiDAR models. The mean and standard deviation (SD) of the R-squared and RMSE values for the cross validation of the training models is reported**.** The number of samples in the models is represented by the n-values (n = training dataset: testing dataset).

		Training		Testing	
	Forest ecosystem type (Training: validation datasets)	**Mean R^2 ± SD R^2**	**RMSE ± SD (Mg C ha^{-1})**	**R^2**	**RMSE (Mg C ha^{-1})**
2019					
1	Terrestrial forests (primary and secondary) (n = 14109 : 4700)	0.23 ± 0.03	36.81 ± 1.60	0.26	37.24
2	Freshwater swamp forests (n = 467 : 152)	0.38 ± 0.14	30.85 ± 7.31	0.44	28.26
3	Mangroves (n = 1122 : 372)	0.43 ± 0.08	21.43 ± 1.37	0.31	23.97
2014					
1	Terrestrial forests (primary and secondary) (n = 15987 : 5328)	0.29 ± 0.03	37.92 ± 1.58	0.34	36.35
2	Freshwater swamp forests (n = 466 : 152)	0.41 ± 0.13	28.30 ± 6.92	0.39	32.31
3	Mangroves (n = 1474: 488)	0.38 ± 0.06	12.02 ± 0.73	0.41	11.56

Two maps of the predicted ACD in 2014 and 2019 were generated from the Satellite Imagery-LiDAR models (Fig. 7; hereafter referred to as "satellite-predicted ACD"). The mean satellite-predicted ACD in Singapore for 2019 was the highest for terrestrial forests (113.92 Mg C ha^{-1}), followed by freshwater swamp forests (108.25 Mg C ha^{-1}) and mangroves (95.55 Mg C ha^{-1}) (Table 8). In contrast, the highest mean LiDAR-predicted ACD for 2014 were found in freshwater swamp forests (121.66 Mg C ha^{-1}), followed by mangroves (109.18 Mg C ha^{-1}) and terrestrial forests (95.15 Mg C ha^{-1}) (Table 8). The differences in trends of the satellite-predicted ACD for 2014 and 2019 between the forest ecosystem types were similar to their respective LiDAR-predicted ACD. Furthermore, the range in satellite-predicted ACD was the highest for terrestrial forest ecosystems in 2014 (43.74 – 404.37 Mg C ha^{-1}) and 2019 (69.23 – 360.84 Mg C ha^{-1}) (Table 8). Despite these differences, the terrestrial forests models showed consistently high ACD for Bukit Timah Nature Reserve and Central Catchment Nature Reserve with 114.75 – 115.80 Mg C ha^{-1} for 2019 and 106.44 – 110.58 Mg C ha^{-1} for 2014.

The spatial distribution of the satellite-predicted ACD in 2014 and 2019 was similar for all forest ecosystem types (Fig. 7). Areas with the high predicted ACD (>100 Mg C ha^{-1}) were concentrated in the Central Catchment Nature Reserve, Nee Soon Swamp Forest, non-swamp areas of Nee Soon, Bukit Timah Nature Reserve, MacRitchie Nature Trail, Clementi Forest, Sungei Buloh Wetland Reserve, and central area of Pulau Ubin (Fig. 7). In comparison, areas with low predicted ACD (<100 Mg C ha^{-1}) were concentrated in the forest around Western Water Catchment, Sarimbun reservoir, Tengah airbase, and the western part of Tengah (Brickland) (Fig. 7).

The total predicted ACD from the Satellite Imagery-LiDAR models for terrestrial forests, freshwater swamp forests, and mangroves in 2019 were 1.97 Tg C, 0.06 Tg C, and 0.15 Tg C respectively. The total predicted ACD in 2019 for all forest ecosystem types is 2.18 Tg C, equivalent to 4.35% of the totally national emissions of carbon dioxide from fossil fuels in 2021, which is estimated to be 50.09 Tg CO_2 (NEA 2021).

Table 8: Summary statistics of the satellite-predicted ACD and the standard deviation (SD) for the different forest ecosystem types for 2014 and 2019.

	Forest ecosystem type	Mean ± SD ACD (Mg C ha^{-1})	Minimum – Maximum ACD (Mg C ha^{-1})
2019			
1	Terrestrial forests (primary and secondary)	113.92 ± 25.15	69.23 – 360.84
2	Freshwater swamp forests	108.25 ± 25.99	78.27 – 257.22
3	Mangroves	95.55 ± 20.37	35.72 – 143.60
2014			
1	Terrestrial forests (primary and secondary)	95.15 ± 30.22	43.74 – 404.37
2	Freshwater swamp forests	121.66 ± 25.65	86.85 – 244.92
3	Mangroves	109.18 ± 10.75	86.42 – 138.11

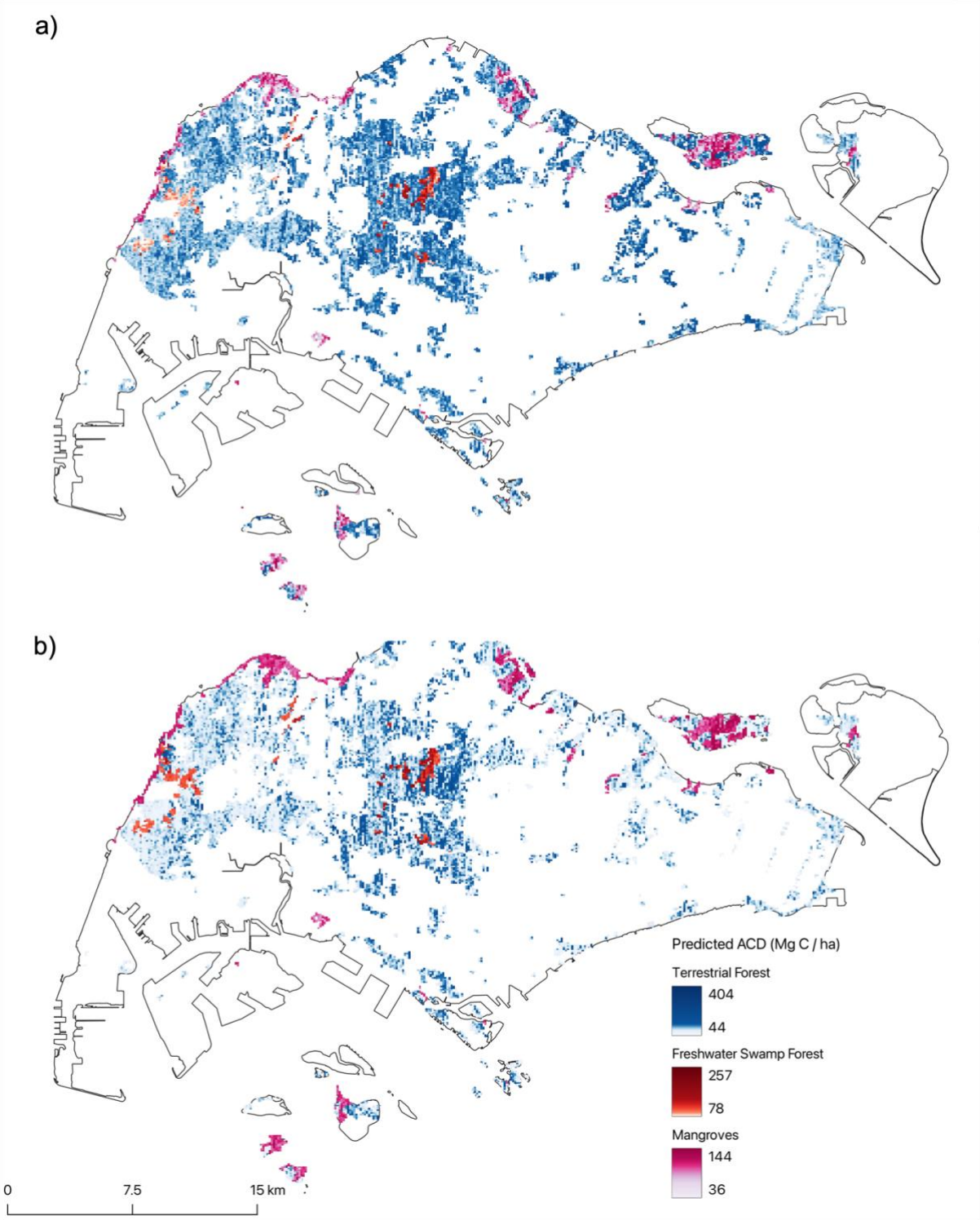

Figure 7: Satellite-predicted ACD for a) 2019 and b) 2014 by forest ecosystem type.

4.4 Comparisons between field-measured and predicted ACD

Through comparing the field-measured ACD, LiDAR-predicted ACD, and satellite-predicted ACD of individual study sites, the 2019 models predicted similar ACD to the actual field measurements (i.e. points close to the identity line) (Fig. 8). However, some of the LiDAR-predicted ACD and satellite-predicted ACD for terrestrial forest sites in 2019 revealed lower values (<300 Mg C ha^{-1}) compared to its respective field-measured ACD (>300 Mg C ha^{-1}) (Fig. 8). For 2014 models, the LiDAR-predicted ACD and satellite-predicted ACD for terrestrial forests showed larger variations of ACD values (i.e. points spread out from the identity line) compared to its associated field-measured ACD (Fig. 8). These differences were also captured in the Tukey pairwise analysis of the field-measured, LiDAR-predicted, and satellite-predicted ACD which showed that only LiDAR-predicted ACD for terrestrial forests were significantly different from the associated field-measured ACD by 33.95 and 65.65 Mg C ha^{-1} for 2019 and 2014 respectively (Table A3; Fig. A5).

Furthermore, the mean LiDAR-predicted ACD (108.34 – 178.99 Mg C ha^{-1}) was higher than the mean field-measured ACD (108.88 – 120.30 Mg C ha^{-1}) and satellite-predicted ACD (94.06 – 127.70 Mg C ha^{-1}) for all forest ecosystem types (Fig. 8 and Table A4). However, the mean field-measured ACD and satellite-predicted ACD for 2014 and 2019 showed similar trends for all forest ecosystem types. For 2019, the mean field-measured and satellite-predicted ACD was the highest for freshwater swamp forests (119.90 – 120.30 Mg C ha^{-1}), followed by terrestrial forest (111.70 – 116.87 Mg C ha^{-1}) and mangroves (94.06 – 108.88 Mg C ha^{-1}) (Table A4). For 2014, the mean field-measured and satellite-predicted ACD was the highest for freshwater swamp forests (120.20 – 127.70 Mg C ha^{-1}), followed by mangroves (107.68 – 118.12 Mg C ha^{-1}) and terrestrial forest (107.01 – 113.34 Mg C ha^{-1}) (Table A4).

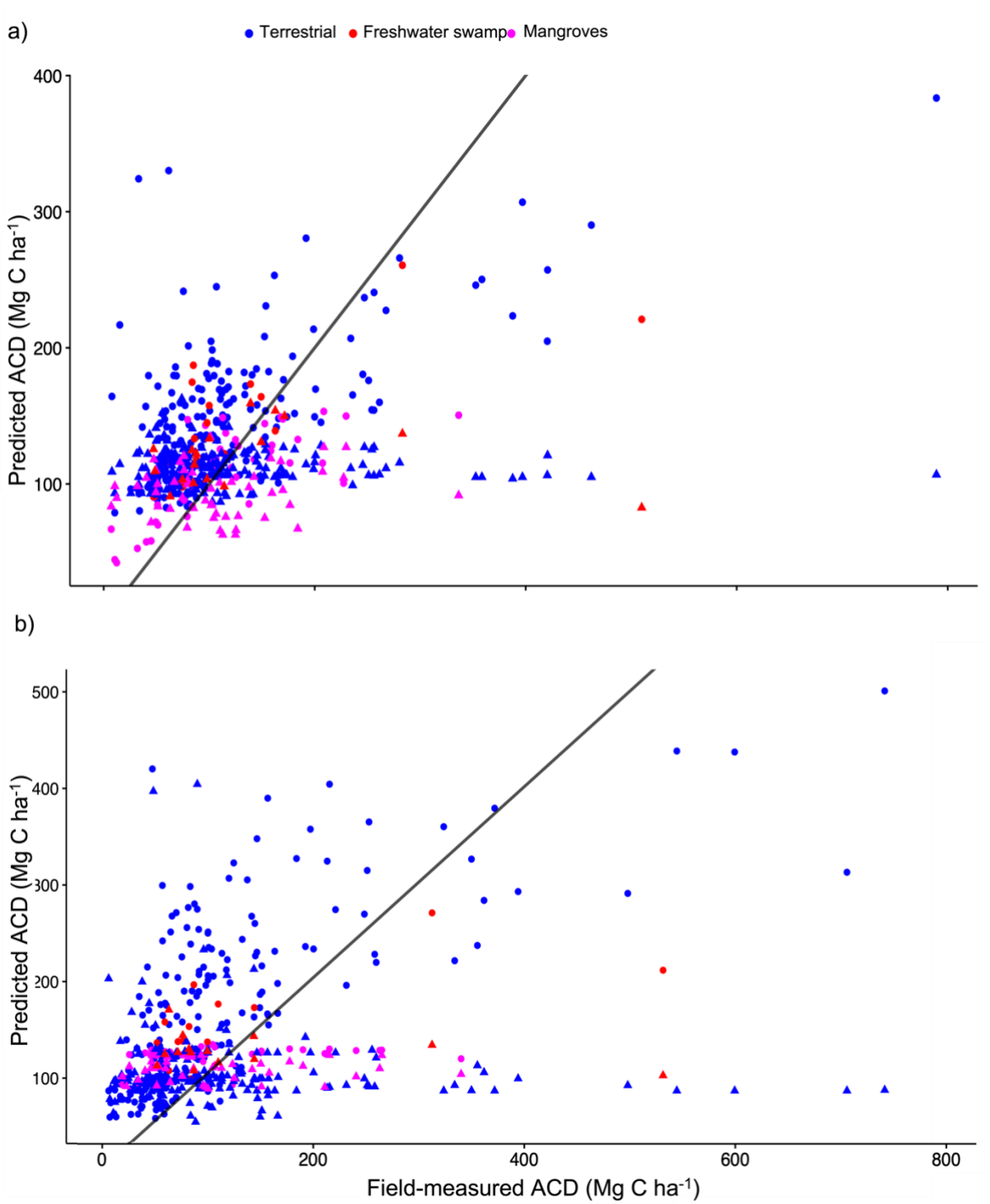

Figure 8: Scatterplots of the field-measured and predicted ACD for all study sites by forest ecosystem type for a) 2019 and b) 2014. The circles and triangles in the plot represent LiDAR-predicted ACD and satellite-predicted ACD respectively. The black line represents the identity (1:1) line, and points clustering close to the line had similar values between the predicted ACD and field-measured ACD.

4.5 Belowground soil carbon in secondary forests

The measurements of belowground soil organic carbon (SOC) were conducted on four secondary forests in Bukit Batok Nature Park (BBNP), Bukit Batok Town Park (BBTP), Windsor Nature Park (WNP), and Thomson Nature Park (TNP).

The mean SOC down to 200 cm for each secondary forest was the highest for BBTP at 140.3 Mg C ha^{-1} and the lowest for BBNP at 81.7 Mg C ha^{-1} (Table 9). WNP and TNP sites showed similar mean SOC down to a depth of 200 cm at 95.2 Mg C ha^{-1} and 99.4 Mg C ha^{-1} respectively (Table 9). However, there were within-site differences in the SOC down to 200 cm between sampling plots (Fig. 9). The highest range of SOC down to 200 cm was found in soil cores collected in BBTP from 77 – 184 Mg C ha^{-1} while the lowest in BBNP from 72 – 76 Mg C ha^{-1} (Fig. 9). The range of SOC down to 200 cm for WNP and TNP were similar with a range of 54 – 113 and 67 – 135 Mg C ha^{-1} respectively (Fig. 9).

The high total SOC in BBTP compared to other secondary forest was due to higher mean SOC (36.3 Mg C ha^{-1}) measured in the 100 – 150 cm depth interval compared to the other sites (10.2 – 14.4 Mg C ha^{-1}) (Table 9). Furthermore, there was a general increasing trend of mean SOC from 9.7 – 15.2 Mg C ha^{-1} at 30 - 50 cm to 19.7 – 30.5 Mg C ha^{-1} at the surface soil in all secondary forests (Table 9).

Table 9: Comparison of mean SOC at each depth interval and sum down to 100 cm, 150 cm and 200 cm between the study sites.

	Mean SOC (Mg C ha^{-1})			
Depth Intervals (cm)	BBNP	BBTP	WNP	TNP
0 – 10 (surface)	19.7	30.5	21.0	30.1
10 – 30	12.1	26.1	18.6	17.4
30 – 50	14.3	15.2	11.2	9.7
50 – 100	17.9	23.3	19.8	21.3
100 – 150	10.2	36.3	14.4	13.0
150 – 200	7.5	8.9	10.2	7.9
	Sum SOC (Mg C ha^{-1})			
Down to 100 cm	**64.0**	**95.1**	**70.6**	**78.5**
Down to 150 cm	**74.2**	**131.4**	**85.0**	**91.5**
Down to 200 cm	**81.7**	**140.3**	**95.2**	**99.4**

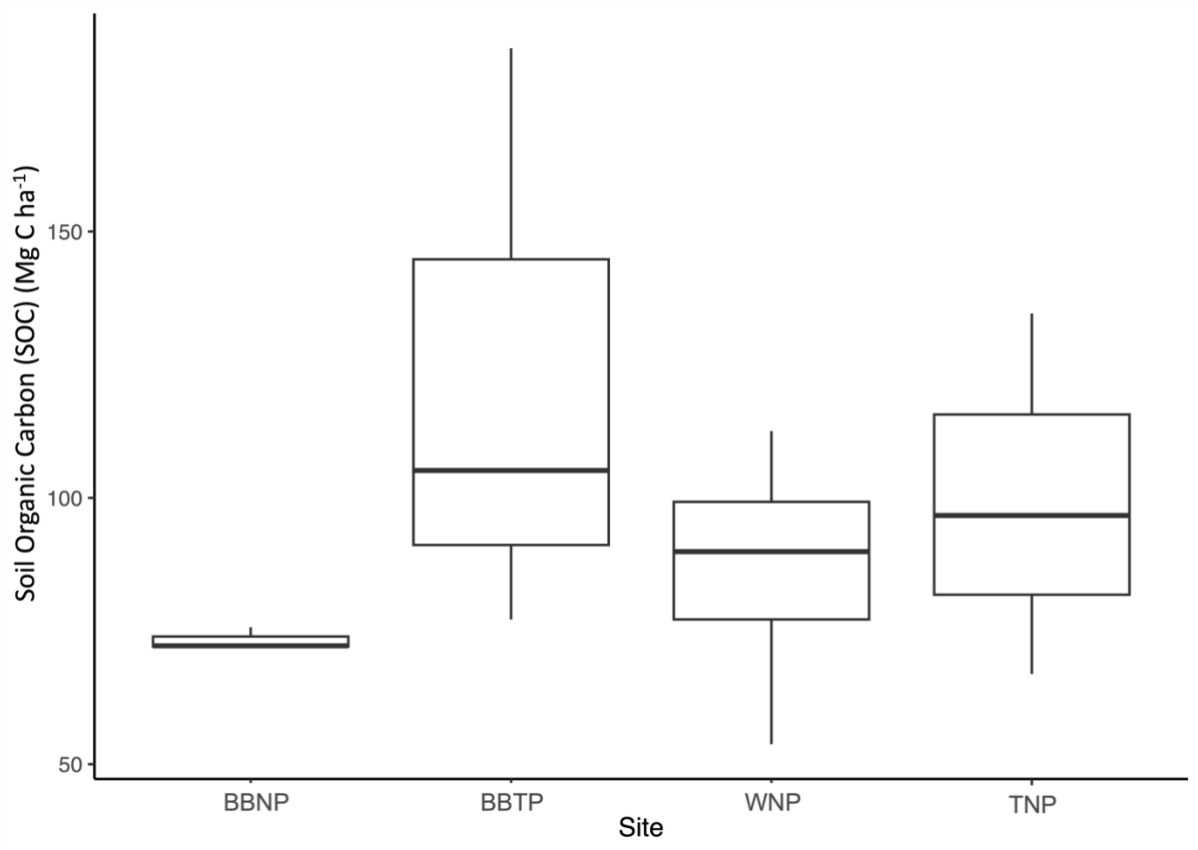

Figure 9: Boxplot showing the distribution of total SOC down to 200 cm for all soil cores obtained from each site.

5. SYNTHESIS

5.1 Comparisons to other tropical forest studies

The mean of the field-measured ACD for terrestrial forests, freshwater swamp forests, and mangroves in Singapore were comparable to some pristine and disturbed forests in other tropical countries (Table 10). For terrestrial forests, the field-measured and LiDAR-predicted ACD values (~100 Mg C ha^{-1}) were similar to a pristine floodplain forest in Brazil (de Assis et al. 2019) and a logged lowland dipterocarp forest in Indonesia (Kronseder et al. 2012). However, the predicted ACD (from both LiDAR and satellite-based models) was low compared to pristine lowland forests in Indonesia and Malaysia (~250 Mg C ha^{-1}) (Kronseder et al. 2012; Seo et al. 2014). On the other hand, freshwater swamp forests showed similar mean ACD (>100 Mg C ha^{-1}) compared to other disturbed swamp forests in Indonesia, but were lower than freshwater swamp forests in Nigeria (~200 Mg C ha^{-1}) (Kronseder et al. 2012; Saragi-Sasmito et al. 2019; Igu & Marchant 2016). The mangroves in Singapore also had comparable ACD (97.90 – 108.88 Mg C ha^{-1}) to mangroves in Malaysia and Nigeria (Igu & Marchant 2016; Hatta et al. 2022).

Table 10: Comparing the means of the field-measured and LiDAR-predicted ACD for this study to similar ecosystem types in other tropical countries.

Study	Forest ecosystem types	Locality	Mean ACD (Mg C ha^{-1})
Singapore (this project)	Terrestrial	Singapore (2019) using field measurements	116.87
		Singapore (2019) using LiDAR-Carbon models	116.61
de Assis et al., 2019		Pristine floodplain forest, Juruá, Brazil	133.98
de Assis et al., 2019		Pristine floodplain forest, Tefé, Brazil	84.65
Kronseder et al., 2012		Unlogged lowland dipterocarp forest, Central Kalimantan, Indonesia	259.87
Kronseder et al., 2012		Logged lowland dipterocarp forest, Central Kalimantan, Indonesia	109.63
Seo et al., 2014		Tangkulap Forest Reserve (FR), Sabah, Malaysian Borneo	255.10
Singapore (this project)	Freshwater swamp	Singapore (2019) using field measurements	120.30
		Singapore (2019) using LiDAR- Carbon models	112.41
Saragi-Sasmito et al., 2018		Secondary peat swamp forest, Central Kalimantan, Indonesia (Northern plot)	118.20
Saragi-Sasmito et al., 2018		Secondary peat swamp forest, Central Kalimantan, Indonesia (Southern plot)	97.60
Igu & Marchant, 2016		Undisturbed freshwater swamp forest, Otuwe, Niger Delta, Nigeria	228.28
Igu & Marchant, 2016		Disturbed freshwater swamp forest, Akili-Ogidi, Niger Delta, Nigeria	134.30

Kronseder et al., 2012		Unlogged peat swamp forest, Central Kalimantan, Indonesia	108.35
Kronseder et al., 2012		Logged peat swamp forest, Central Kalimantan, Indonesia	75.95
Singapore (this project)	Mangrove	Singapore (2019) using field measurements	108.88
		Singapore (2019) using LiDAR-Carbon models	97.90
Mhd Hatta et al., 2019		Kudat's Tun Mustapha Park mangrove forest, Sabah, Malaysia.	136.58
Igu & Marchant, 2016		Freshwater-mangrove transition secondary forest, Akoloma, Niger Delta, Nigeria	100.69

A comparison between LiDAR-Carbon models from this study and other aboveground carbon studies in tropical Asia showed that RF models sometimes have lower performance compared to multiple linear regression models, but relatively high predictive accuracy (Table 11) (Yang et al. 2012; Chan et al. 2021; Jha et al. 2020). Using similar LiDAR metrics and RF models, Yang et al. (2012) found that R^2 values of RF models increased with larger area extent of study plots but emphasized that the use of multiple LiDAR metrics can either improve estimation accuracy or add more noise to the final model. In addition, Chan et al. (2021) and Jha et al. (2020) used multiple linear regression with leave-one-out cross-validation (LOOCV) to filter out important LiDAR metrics (e.g. top of canopy height) for the final ACD model which resulted in much higher R^2 and lower RMSE values (Table 11). These comparisons suggest the importance of filtering redundant LiDAR metrics to remove noise and improve model performance.

Table 11: Comparison of LiDAR-Carbon model performance between this study and existing literature for forest ecosystem types in Asia.

Study	Forest ecosystem type	Locality	Plot design	LiDAR information	Final LiDAR metrics used in the model	Models used	R^2 value and RMSE values of the models	Remarks/Comments
This project	Terrestrial forests; Freshwater swamp forest; Mangroves	Singapore	2019: Terrestrial forests: 7.2 ha Freshwater swamp forest: 1.60 ha Mangroves: 0.77 ha 2014: Terrestrial forests: 7.88 ha Freshwater swamp forest: 1.60 ha Mangroves: 0.60 ha	Airborne LiDAR using long-range LiDAR scanning system and incorporated into the Global Positioning System-Inertial Measurement Unit (GPS-IMU).	21 LiDAR height and canopy metrics	Random Forest models. Models were trained and tested using 75% and 25% split in datasets.	2019: Training models: R^2 from 0.33 – 0.64 and RMSE of 45 – 78 Mg C ha^{-1} Testing data: R^2 from 0.31 – 0.45 and RMSE from 67 – 72 Mg C ha^{-1} 2014: Training models: R^2 of 0.49 – 0.74 and RMSE of 62 – 81 Mg C ha^{-1} Testing data: R^2 from 0.15 – 0.34 and RMSE from 42 – 70 Mg C ha^{-1}	
Yang et al., 2022	Tropical broadleaf forest	China	400 plots (0.04 ha each – 1,082 ha in total)	UAV LiDAR data equipped with a RIEGL VUX-1 UAV laser scanner (RIEGL Laser Measurement Systems, Horn, Austria).	Maximum, mean and standard deviation of canopy height and coefficient of variation of canopy height	Random Forests models. Models were trained and tested using the same field measurements plots.	Training models: R^2 from 0.10 – 0.30, RMSE from 120 – 180 Mg C ha^{-1} depending on the number of plots. Testing data: R^2 of 0.53 and RMSE of 118.38 Mg C ha^{-1}	This study had many different sites and used many different methods to compare the relationship between LiDAR and Satellite imageries metrics. Only relevant data are summarised in this table.

Chan et al., 2021	Subtropical terrestrial forest	Hong Kong	1 ha forest plot (demarcated by 25 quadrats in 20 m × 20 m and further sub-divided into sixteen 5 m × 5 m sub-quadrats)	Airborne LiDAR was captured by Optech Gemini ALTM Airborne Laser Terrain Mapper	Raw LiDAR point cloud was pre-processed to normalized height point cloud to generate the LiDAR metric	Multiple linear regression models using Leave-one-out cross validation (LOOCV). Bootstrapping was adopted to assess statistical accuracy in terms of the confidence intervals.	R^2 of 0.864 and RMSE of 37.75 Mg C ha^{-1}	LiDAR metrics was extracted at 10 m radius size and field-measured ACD was resampled at similar size to obtain the best model.
Jha et al., 2020	Terrestrial forest (deciduous)	Khao Yai National Park, Thailand	1) 30 ha contiguous forest (500 m × 600 m). 2) Eight separate 0.48 ha plots (60 m × 80 m). 3) 1 ha plot (100 m × 100 m) plot	The airborne laser scanning (ALS) campaign was acquired with a RIEGL LMS Q680i installed into a Diamond Aircraft "Airborne Sensors" DA-42 fixed-wing airplane.	Mean of top-of-canopy height (TCH, defined as the maximum height of 1m resolution pixels)	Log–log regression model with leave-one-out cross-validation (LOOCV) scheme to select the most predictive lidar metrics.	R^2 of 0.85 and RMSE of 45 Mg C ha^{-1}	LiDAR metrics and field-measured ACD was resampled at 0.5 ha scale to obtain the best model.

The mean soil organic carbon (SOC) down to 200 cm measured in this project for exotic-dominated secondary forests in BBNP, BBTP, WNP, and TNP (81.7 – 140.3 Mg C ha^{-1}) were comparable to other primary and native-dominated secondary forests in Singapore such as the non-swamp areas of Nee Soon (167.9 Mg C ha^{-1}) and Bukit Timah Nature Reserve (BTNR) (99.2 – 127.7 Mg C ha^{-1}) (Fig. 10 and Table 9) (Ngo et al., 2013). Comparing to the other forest ecosystem types, the mean SOC down to 200 cm in freshwater swamp forest in Nee Soon was almost 4 times more than terrestrial forests at 528.1 Mg C ha^{-1} (Fig.10) (NParks, 2018). The mangroves in Chek Jawa also showed very high mean SOC down to 100 cm at 307.0 Mg C ha^{-1} (Fig. 10) (Phang et al., 2015). Additionally, there was a consistent increase in SOC from 50 cm to the soil surface in all terrestrial and freshwater swamp forest ecosystems in Singapore suggests the possible benefits of rehabilitation of secondary vegetation after the abandonment of previous land use such as plantation, villages, and quarries in 1980s (Fig.10 and Table 9) (Yee et al. 2019; Wee & Corlett 1986).

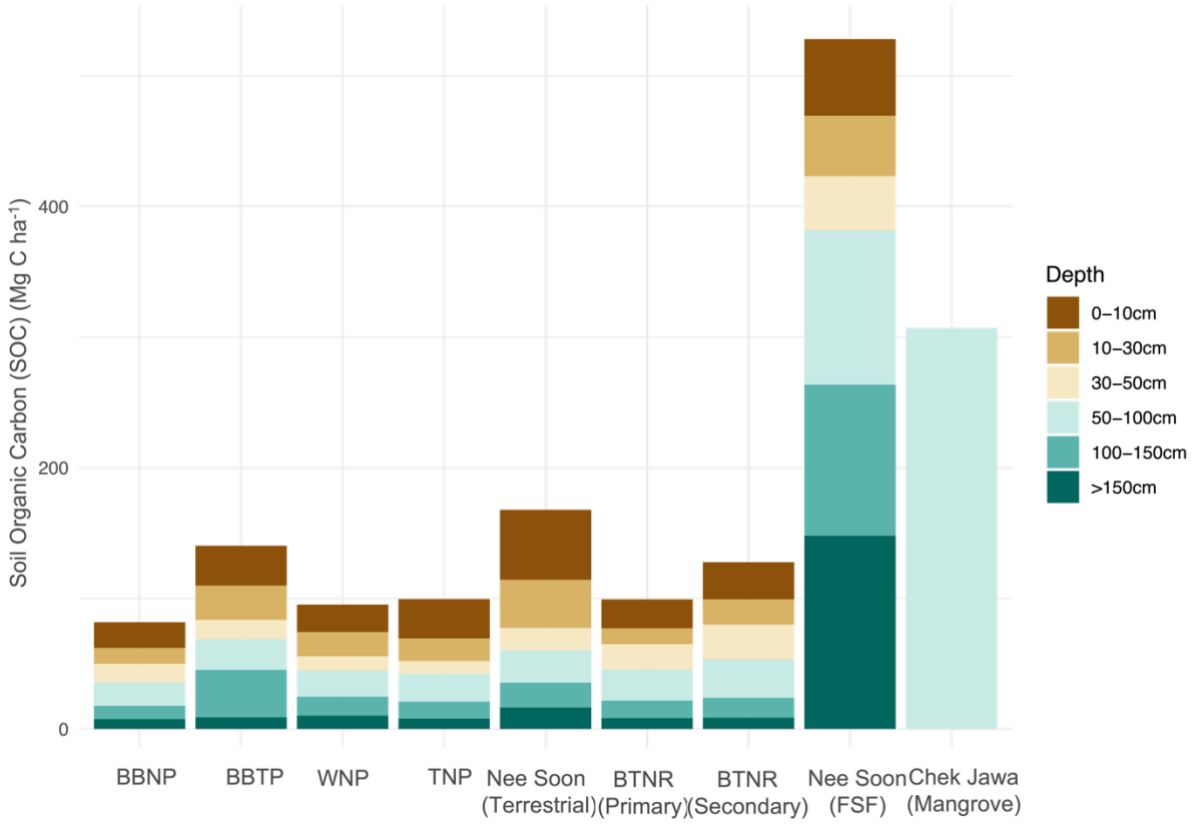

Figure 10: Mean sum of SOC down to 200 cm for secondary terrestrial forests in BBNP, BBTP, WNP, and TNP conducted for this project, terrestrial forest in non-swamp areas of Nee Soon (NParks, 2018), primary and secondary terrestrial forests in Bukit Timah Nature Reserve (BBTNR) (Ngo et al., 2013), freshwater swamp forest (FSF) in Nee Soon (NParks, 2018), and mangroves in Chek Jawa (Phang et al., 2015). For mangroves in Chek Jawa, the mean SOC presented here is the total value down to 100 cm as no information were provided for each depth (Phang et al., 2015).

5.2 Application of the project findings

Our project provided a preliminary estimate of the ACD for different forest ecosystem types across Singapore and demonstrated the use of remote sensing technology for potential monitoring of forest ACD. We showed that remote sensing technology can generate ACD predictions that are similar to field-measured ACD (Fig. 8). Further, we demonstrate that remote sensing technology can be used to scale up field measurements and estimate spatially explicit ACD over a larger area. The small difference in ACD values between field-measurements, LiDAR predictions, and satellite predictions (Fig. 8 and Table A4) consolidates the need for multidisciplinary projects such as this one to make well-informed conservation decisions. Moreover, our carbon maps estimated using the complete LiDAR and satellite coverage of Singapore enable precise location of areas of interest to protect or invest in, as well as areas with highly different carbon estimations that need further investigation.

There were, however, key knowledge gaps identified in the methodology that necessitate additional study. For example, optical and radar satellites are less sensitive in areas of high biomass, resulting in a possible underestimation of ACD in areas of dense forest (Table A4). This has been observed in other forest biomass studies, caused by a saturation of signals or spectral reflectance at higher biomass (Joshi et al. 2017; Mutanga et al. 2023). The issue can be potentially mitigated by using a hybrid of LiDAR with optical or radar satellite data that have different spatial and spectral information (Mutanga et al. 2023). Care should also be taken in the sampling design of the field measurements used to calibrate the models. Factors such as plot size, shape, and number may all play a role in influencing the accuracy of the results (Meyer et al. 2013). Likewise, the selection of model parameters is subjected to the type and structure of the data (e.g. ratio of independent variables to dependent variables, variability of the data) and should be set according to the specific datasets.

Finally, the applicability of the modelling framework has only been tested on forest ecosystem types in Singapore. Given the diversity of forest ecosystem types and land use history in Southeast Asia, the applicability of the modelling framework would greatly benefit from incorporating additional data from other forest ecosystem types in the region. Moving forward, we recommend collecting forest inventory data from other tropical forests in Southeast Asia to examine the spatial transferability of the models and modelling framework, in addition to the usefulness of remote sensing in scaling of ACD estimates over larger areas.

6. LIMITATIONS AND MITIGATIVE ACTIONS

Several methodological limitations may have contributed to the current level of model performance (Table 12). As this project used Singapore as a testbed to explore methods to improve carbon monitoring of forest ecosystem types, the mitigative actions listed here will be part of NUS CNCS's future studies in Southeast Asia.

Table 12: Methodological limitations and mitigative actions for improving carbon monitoring of tropical forest ecosystem types.

	Limitations of the current methodology	Mitigative actions
1	Using one land use map (Gaw et al. 2019) for the 2014 and 2019 models to determine the areas of different forest ecosystem types could have resulted in the over- or underestimation of the forest areas and subsequent ACD calculations. As the landscape of Singapore is continually changing, the areas of all forest ecosystem types can change rapidly between 2011 and 2023 (different periods of field-measured ACD).	Develop a vegetation map of the three forest ecosystem types using LiDAR and satellite data for 2014 to ensure accurate forest area and ACD calculations.
2	Temporal mismatches in the date of collection for field and LiDAR data could contribute to poor model performance. Using different sampling sites for forest inventory measurements for 2014 and 2019 could contribute to different model outputs.	Plan field and remote sensing campaigns in conjunction where possible. For multi-year comparisons, ensure sampling sites for forest inventory measurements are similar such that model outputs are consistent and comparable.
3	21 LiDAR metrics were extracted from the point clouds following the literature (Yang et al. 2012). However, these parameters were likely correlated, leading to fluctuations in model.	Perform further multicollinearity tests to avoid highly collinear variables and select variables more intentionally according to information theoretic approaches. Alternatively, other LiDAR metrics such as top of canopy height and other ratios can also be considered.
4	Small sample sizes and clustered plots for freshwater swamp forests and mangroves could result in biased representation of the respective forest ecosystem types and possibly inflating the R^2 values of the training models.	Incorporate spatial autocorrelation into the models to account for partial clustering in the plots. Where possible, collect additional field measurements in undersampled areas of mangroves and freshwater swamp forests to ensure that local variations in ACD can be captured.
5	Subsuming primary and secondary forests under a terrestrial forest category contributed to higher-than-expected variations in the ACD. As such, the terrestrial forest models had lower performance compared to other forest ecosystem types.	New vegetation maps with finer forest classifications may help in reducing the variation per forest ecosystem type. For example, Yee et al. (2016) showed that secondary forests in Singapore can be further classified into a) native-dominated/regrowth secondary forests, b) exotic-dominated/abandoned-land forests, and c) waste woodlands. Subsequently, multiple ecosystem-specific models can be developed that better represent the forest ecosystem types.

7. SUMMARY

In summary, the project developed aboveground carbon density (ACD) maps of three forest ecosystem types (terrestrial forest, freshwater swamp forest, and mangrove forest) in Singapore, while providing preliminary belowground soil carbon estimates for some secondary forest sites. The key findings are:

- Based on field measurements, freshwater swamp forests are the most carbon dense forest ecosystem in Singapore. All models predicted higher mean ACD for freshwater swamp forests (108.25 – 125.21 megagram of biomass carbon per hectare (Mg C ha^{-1}) and terrestrial forests (95.15 – 116.61 Mg C ha^{-1}) compared to mangroves (95.55 – 109.18 Mg C ha^{-1}).
- The forest ecosystems in Singapore store substantial amount of aboveground carbon. The models estimate 1.37 – 2.18 teragram of aboveground biomass carbon (Tg C) across the 14,930 ha of forests in Singapore in 2019. This equals to 2.74 – 4.35% of the 2021 national CO2 emissions from fossil fuels.
- Our models partially explain the variation in ACD with the best performance for LiDAR-based models of freshwater swamp forests (R^2 = 0.64 – 0.74), followed by mangroves (R^2 = 0.54 – 0.60) and terrestrial forests (R^2 = 0.33 – 0.49).
- Exotic-dominated secondary forests play a role in carbon sequestration and contribute to belowground soil organic carbon (SOC) of 81.7 – 140.3 Mg C ha^{-1}. This was comparable to the SOC documented in other terrestrial forests in the non-swamp areas of Nee Soon (~167.9 Mg C ha^{-1}) and Bukit Timah Nature Reserve (~99.2 – 127.7 Mg C ha^{-1}) but was lesser than Nee Soon swamp (~528.1 Mg C ha^{-1}) and mangroves in Chek Jawa (~307.0 Mg C ha^{-1}).

Moving forward, we will collaborate with the broader research community and partners like HSBC to continuously improve the methodologies and predicted ACD maps for the different forest ecosystem types, which will lead to improved spatially explicit information on the distribution of carbon across Singapore for land use planning and conservation purposes.

8. ACKNOWLEDGEMENTS

The “Singapore Project” is implemented by the Centre for Nature-based Climate Solutions at the National University of Singapore in collaboration with the Singapore Land Authority (SLA) and National Parks Board (NParks). Funding support for the project is kindly provided by Hongkong and Shanghai Banking Corporation Limited, Singapore (HSBC).

The Bukit Timah tree dataset was supported by the Forest Global Earth Observatory (ForestGEO) of the Smithsonian Tropical Research Institute (STRI), the National Institute of Education, Nanyang Technological University, the Arnold Arboretum of Harvard University, and the National Parks Board of Singapore. In addition, we would like to thank the various researchers who have kindly provided us the forest inventory data: Zoë Shribman, Dr. Dan Friess, Dr. Shawn Lum, and Dr. Kang Min Ngo.

9. REFERENCES

De Alban JDT et al. (2018) Combined Landsat and L-band SAR data improves land cover classification and change detection in dynamic tropical landscapes. Remote Sensing 10

Asner GP, Mascaro J (2014) Mapping tropical forest carbon: Calibrating plot estimates to a simple LiDAR metric. Remote Sensing of Environment 140:614–624

de Assis RL et al. (2019) Above-ground woody biomass distribution in Amazonian floodplain forests: Effects of hydroperiod and substrate properties. Forest Ecology and Management 432:365–375

Bode M et al. (2015) A conservation planning approach to mitigate the impacts of leakage from protected area networks. Conservation Biology 29:765–774

Breiman L (2001) Random forests. Machine Learning 45:5–32

Cai Y et al. (2018) Conservation outputs and recommendations for Nee Soon freshwater swamp forest, Singapore. Gardens' Bulletin Singapore 70:191–217

Chan EPY, Fung T, Wong FKK (2021) Estimating above-ground biomass of subtropical forest using airborne LiDAR in Hong Kong. Scientific Reports 11:1–14

Chave J et al. (2014) Improved allometric models to estimate the aboveground biomass of tropical trees. Global Change Biology 20:3177–3190

Chave J et al. (2009) Towards a worldwide wood economics spectrum. Ecology Letters 12:351–366

Chong KY et al. (2021) Waterlogging and soil but not seedling competition structure tree communities in a catchment containing a tropical freshwater swamp forest. Journal of Vegetation Science 32:1–11

Csillik O et al. (2019) Monitoring tropical forest carbon stocks and emissions using Planet satellite data. Scientific Reports 9:1–12

Er KBH et al. (2023) Establishing a network of long-term forest monitoring plots in Singapore. Gardens' Bulletin Singapore 75:1–20

Friess DA, Richards DR, Phang VXH (2016) Mangrove forests store high densities of carbon across the tropical urban landscape of Singapore. Urban Ecosystems 19:795–810

Gaw LYF, Yee ATK, Richards DR (2019) A high-resolution map of Singapore's terrestrial ecosystems. Data 4:1–10

Gorelick N et al. (2017) Google Earth Engine: Planetary-scale geospatial analysis for everyone. Remote Sensing of Environment 202:18–27

Graves S et al. (2023) multcompView. 1–24

Greenfield P (2023) Revealed: more than 90% of rainforest carbon offsets by biggest certifier are worthless, analysis shows. The Guardian

Griscom BW et al. (2017) Natural climate solutions. Proceedings of the National Academy of Sciences of the United States of America 114:11645–11650

Haralick RM, Dinstein I, Shanmugam K (1973) Textural features for image classification. IEEE Transactions on Systems, Man and Cybernetics SMC-3:610–621

Harris D, Horwáth WR, van Kessel C (2001) Acid fumigation of soils to remove carbonates prior to total organic carbon or CARBON-13 isotopic analysis. Soil Science Society of America Journal 65:1853–1856

Hatta SM et al. (2022) Estimation of carbon pool at mangrove forest of Kudat, Sabah, Malaysia. Biodiversitas 23:4601–4608

Igu NI, Marchant R (2016) Aboveground carbon storage in a freshwater swamp forest ecosystem in the Niger Delta. Carbon Management 7:137–148

IPCC (2006) IPCC Guidelines for National Greenhouse Gas Inventories: Agriculture, Forestry and Other Land Use. Hayama

Isenburg M (2014) LAStools.

IUCN (2024) About Nature-based Solutions.

Jha N et al. (2020) Forest aboveground biomass stock and resilience in a tropical landscape of Thailand. Biogeosciences 17:121–134

Joshi N et al. (2017) Understanding 'saturation' of radar signals over forests. Scientific Reports 7:1–11

Jucker T et al. (2022) Tallo: A global tree allometry and crown architecture database. Global Change Biology 28:5254–5268

Kauffman JB, Donato DC (2012) Protocols for the measurement, monitoring and reporting of structure, biomass and carbon stocks in mangrove forests. Bogor

Koh LP et al. (2021) Carbon prospecting in tropical forests for climate change mitigation. Nature Communications 12:1–9

Kronseder K et al. (2012) Above ground biomass estimation across forest types at different degradation levels in central kalimantan using lidar data. International Journal of Applied Earth Observation and Geoinformation 18:37–48

Kuhn M et al. (2016) caret: Classification and regression training.

Lai HR et al. (2021) Decoupled responses of native and exotic tree diversities to distance from old-growth forest and soil phosphorus in novel secondary forests. Applied Vegetation Science 24:1–11

Lai HR et al. (2020) Functional traits that moderate tropical tree recruitment during post-windstorm secondary succession. Journal of Ecology 108:1322–1333

Meyer V et al. (2013) Detecting tropical forest biomass dynamics from repeated airborne lidar measurements. Biogeosciences 10:5421–5438

Mutanga O, Masenyama A, Sibanda M (2023) Spectral saturation in the remote sensing of high-density vegetation traits: A systematic review of progress, challenges, and prospects. ISPRS Journal of Photogrammetry and Remote Sensing 198:297–309

NEA (2021) Greenhouse Gas Inventory.

NEA (2020) Singapore's Fourth Biennial Update Report Under The United Nations Framework Convention On Climate Change. Singapore

Neo L et al. (2017) Vascular plant species richness and composition in two types of post-cultivation tropical secondary forest. Applied Vegetation Science 20:692–701

Ngo KM et al. (2013) Carbon stocks in primary and secondary tropical forests in Singapore. Forest Ecology and Management 296:81–89

Ngo KM et al. (2016) Resilience of a forest fragment exposed to long-term isolation in Singapore. Plant Ecology and Diversity 9:397–407

Nguyen CTT et al. (2022) Environmental change since the Last Glacial Maximum: palaeo-evidence from the Nee Soon Freshwater Swamp Forest, Singapore. Journal of Quaternary Science 37:707–719

Phang VXH, Chou LM, Friess DA (2015) Ecosystem carbon stocks across a tropical intertidal habitat mosaic of mangrove forest, seagrass meadow, mudflat and sandbar. Earth Surface Processes and Landforms 40:1387–1400

Probst P, Wright MN, Boulesteix AL (2019) Hyperparameters and tuning strategies for random forest. Wiley Interdisciplinary Reviews: Data Mining and Knowledge Discovery 9:1–19

QGIS.org QGIS Geographic Information System.

Réjou-Méchain M et al. (2017) Biomass: an R Package for Estimating Above-Ground Biomass and Its Uncertainty in Tropical Forests. Methods in Ecology and Evolution 8:1163–1167

Saragi-Sasmito MF et al. (2019) Carbon stocks, emissions, and aboveground productivity in restored secondary tropical peat swamp forests. Mitigation and Adaptation Strategies for Global Change 24:521–533

Sarira TV et al. (2022) Co-benefits of forest carbon projects in Southeast Asia. Nature Sustainability 5:393–396

Seddon N et al. (2020) Nature-based solutions in nationally determined contributions | IUCN Library System. Gland, Switzerland and Oxford, UK: IUCN and University of Oxford.

Seo H et al. (2014) Determining aboveground biomass of a forest eeserve in Malaysian Borneo using K-nearest neighbour method. Journal of Tropical Forest Seminar 26:58–68

Seymour F, Langer P (2021) Consideration of Nature-Based Solutions as Offsets in Corporate Climate Change Mitigation Strategies. World Resources Institute 1–27

Shribman Z et al. (2024) Biophysical controls on mangrove blue carbon distribution in Singapore. in-prep

Shribman Z et al. (2023) Landscape-scale biophysical controls on mangrove blue carbon distribution in Singapore. In: Coastal and Estuarine Research Federation 27th Biennial Conference. Portland.

Team RC (2022) R: A language and environment for statistical computing (4.1.3).

Urbazaev M et al. (2018) Estimation of forest aboveground biomass and uncertainties by integration of field measurements, airborne LiDAR, and SAR and optical satellite data in Mexico. Carbon Balance and Management 13

Wang WY et al. (2022) Remarkable diversity in a little red dot: a comprehensive checklist of known ant species in Singapore (Hymenoptera: Formicidae) with notes on ecology and taxonomy. Asian Myrmecology 15:1–152

Wang Z et al. (2023) A multimodel random forest ensemble method for an improved assessment of Chinese terrestrial vegetation carbon density. Methods in Ecology and Evolution 14:117–132

Wong YK, Ting CP, Bin Ibrahim A (1994) The tree communities of the Central Catchment Nature Reserve, Singapore. The Gardens' bulletin, Singapore. 46:37–78

Yang S et al. (2012) The current status of mangrove forests in Singapore. Proceedings of Nature Society, Singapore's Conference on 'Nature Conservation for a Sustainable Singapore' 99–120

Yee ATK et al. (2019) Short-term responses in a secondary tropical forest after a severe windstorm event. Journal of Vegetation Science 30:720–731

Yee ATK et al. (2016) Updating the classification system for the secondary forests of Singapore. Raffles Bulletin of Zoology 2016:11–21

Yee ATK et al. (2011) The vegetation of Singapore — an updated map. Gardens' Bulletin Singapore 63:205–212

Yommy AS, Liu R, Wu AS (2015) SAR image despeckling using refined lee filter. Proceedings - 2015 7th International Conference on Intelligent Human-Machine Systems and Cybernetics, IHMSC 2015 2:260–265

Zhao K et al. (2018) Utility of multitemporal lidar for forest and carbon monitoring: Tree growth, biomass dynamics, and carbon flux. Remote Sensing of Environment 204:883–897

10. APPENDIX

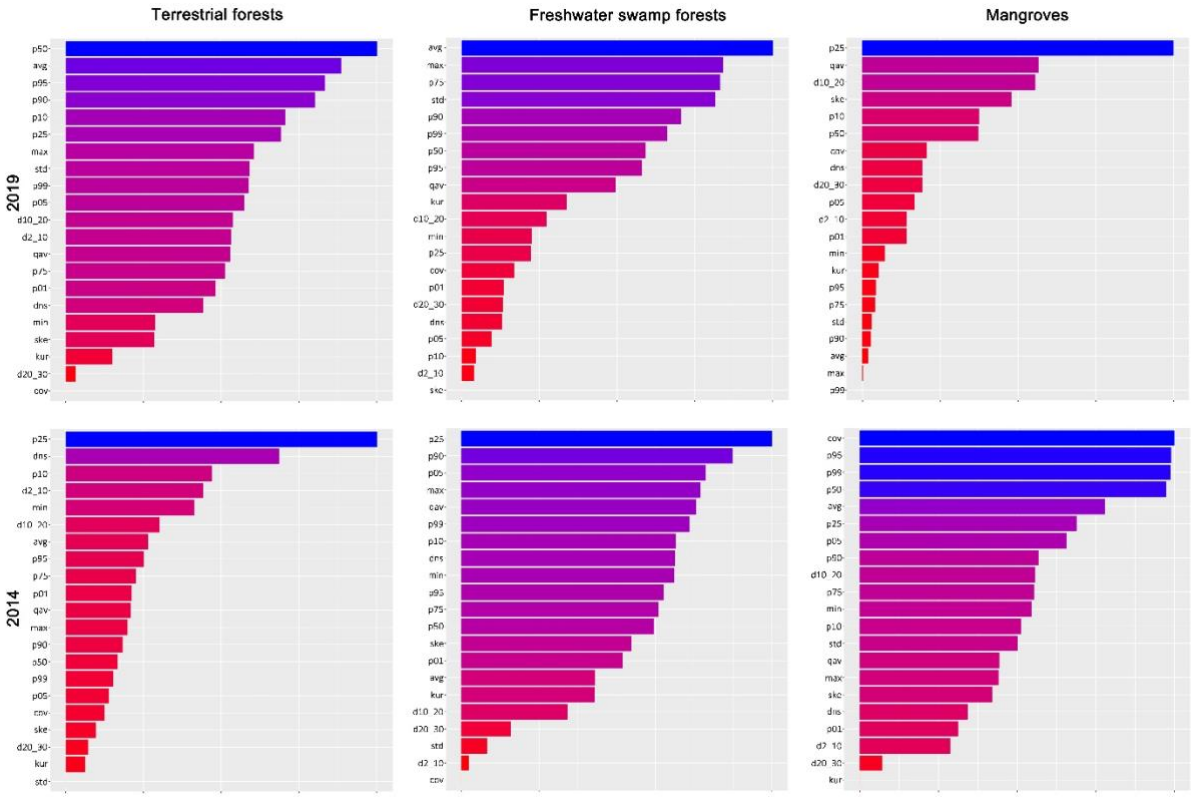

Figure A1: Importance of variables for the LiDAR-Carbon models across all three forest ecosystem types.

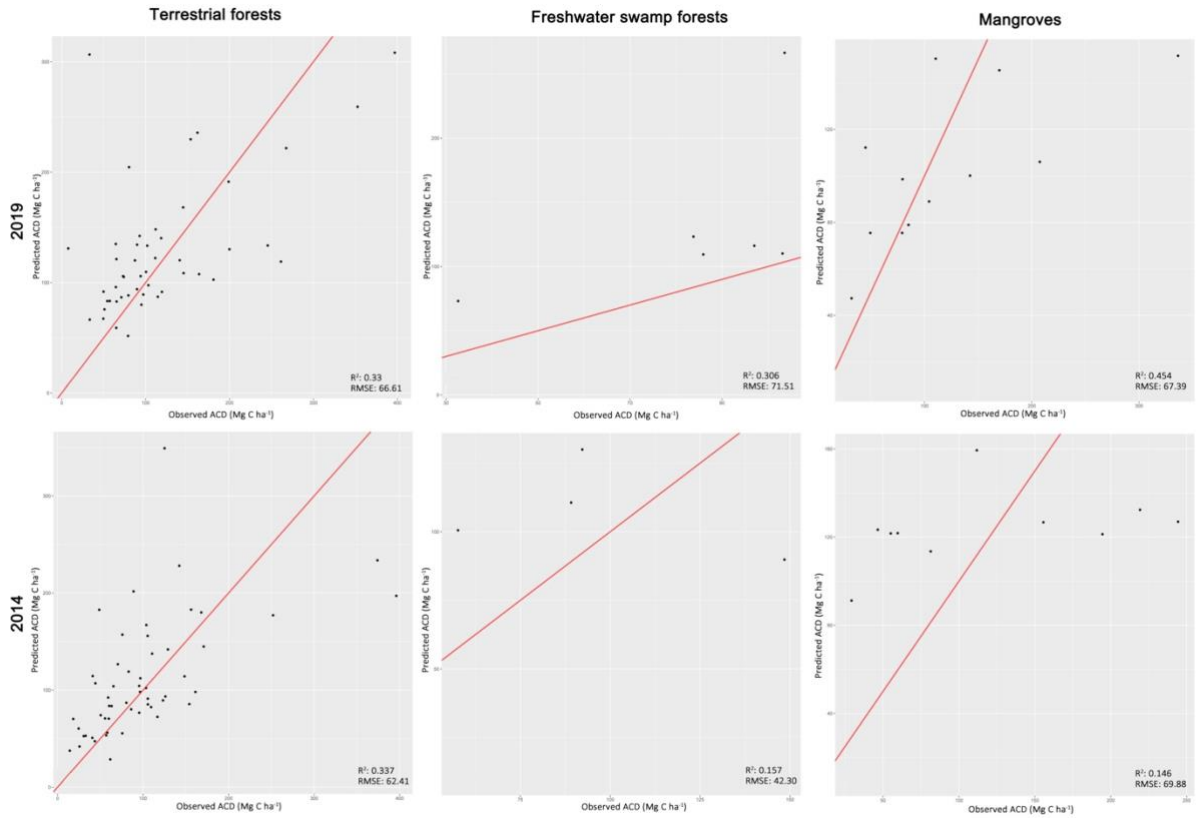

Figure A2: Prediction accuracy of the LiDAR-Carbon models comparing observed ACD in the testing dataset to predicted ACD.

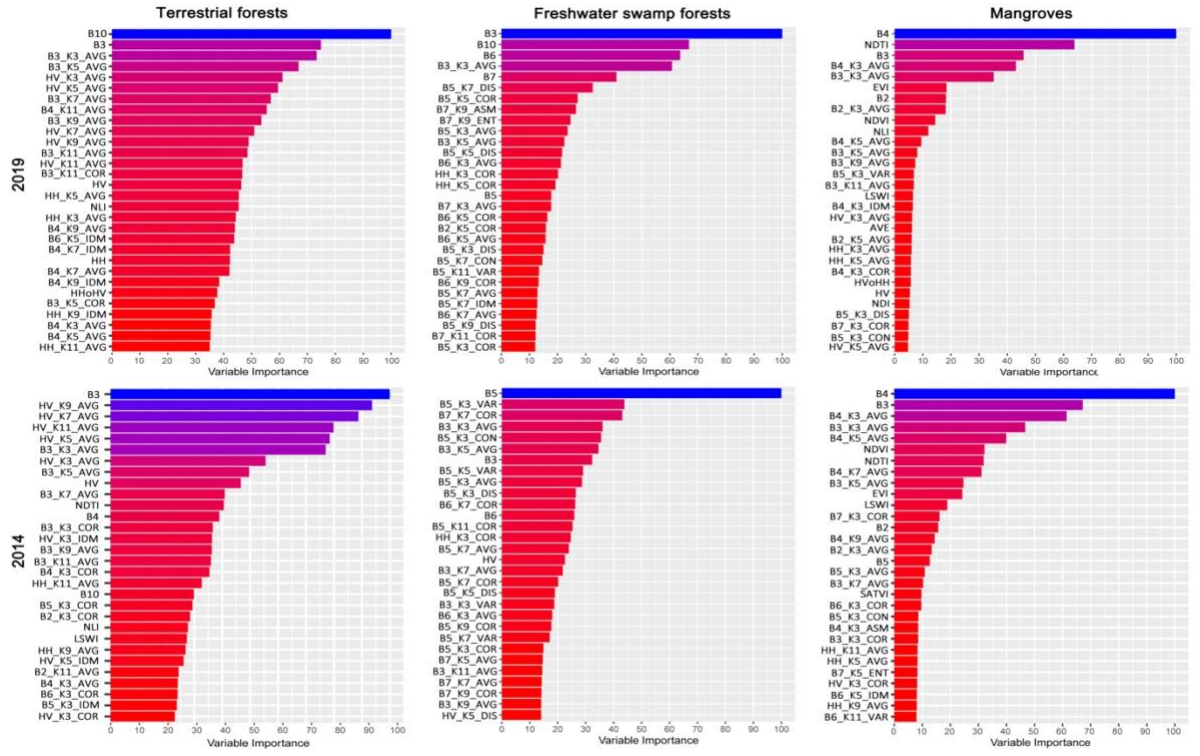

Figure A3: Top 30 most important variables for the Satellite Imagery-LiDAR models across all three forest ecosystem types.

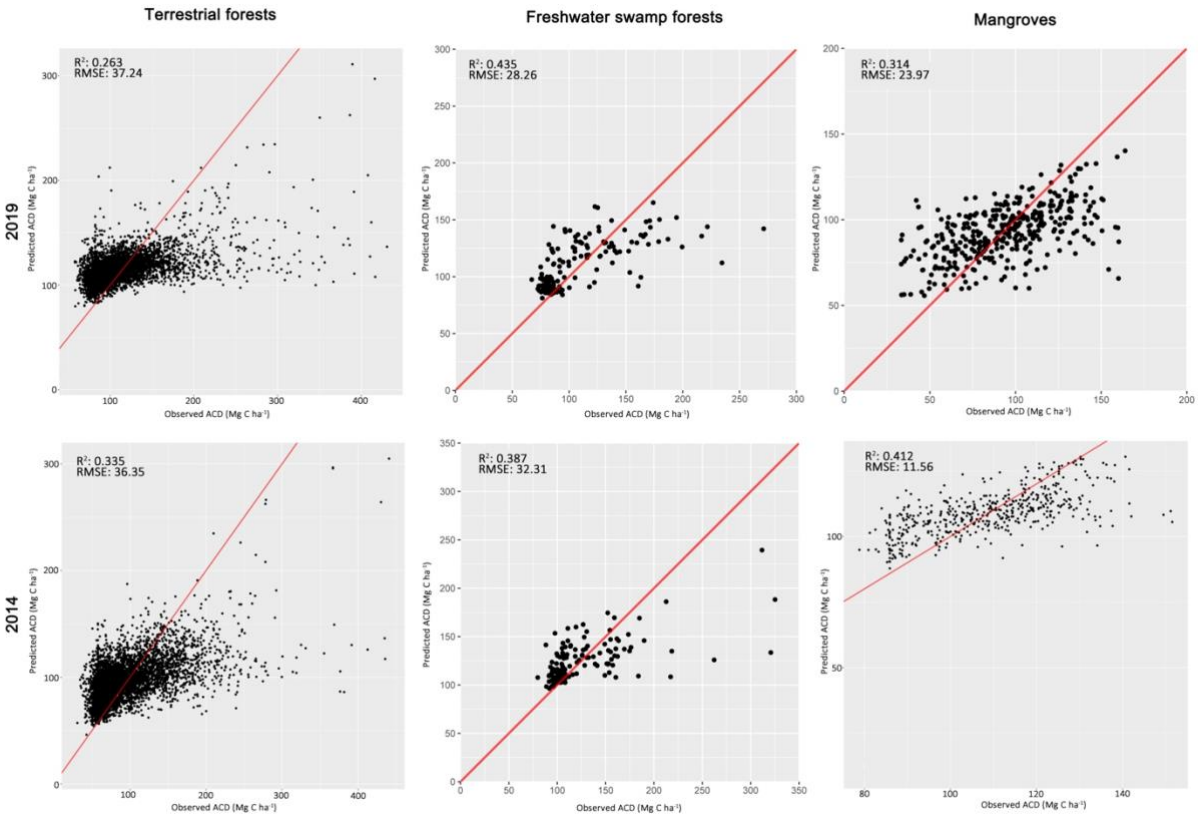

Figure A4: Prediction accuracy of the Satellite Imagery-LiDAR models comparing observed ACD in the testing dataset to predicted ACD.

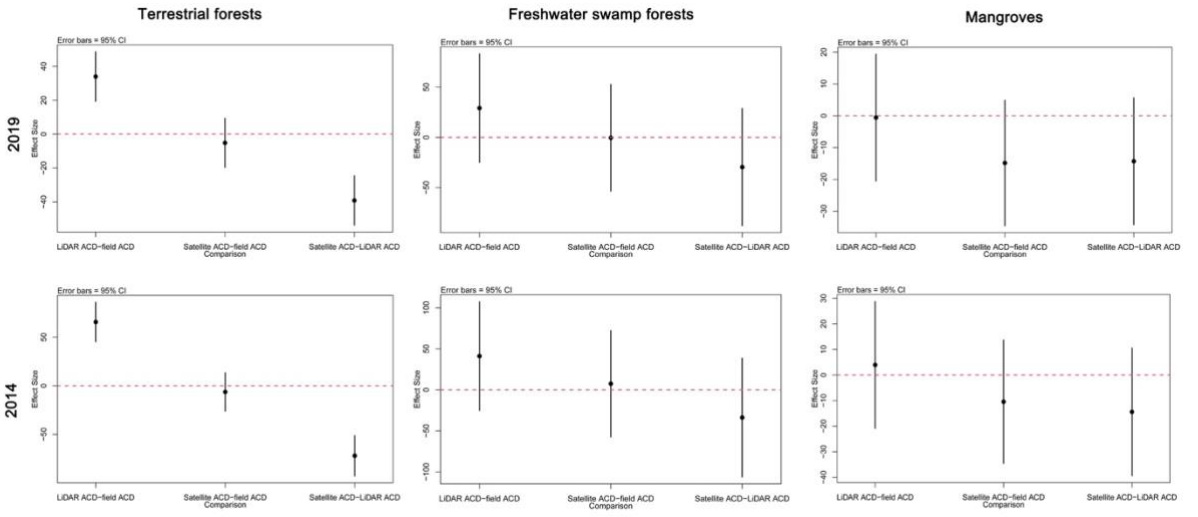

Figure A5: Tukey's test comparison of field-measured and predicted ACD to determine significant difference.

Table A1. Performance of the different height-DBH models. The number of samples (n) in the models corresponds to the number of tree families in each forest ecosystem type.

Forest ecosystem type	Percentage (%) of the respective height models of vegetation (at family level) used to determine the height of trees found in study sites in 2019 based on relationships from Tallo database (Jucker et al. 2022)			
	Weibull	Michaelis	Log1	Log2
Terrestrial forests (n = 71)	76	8	9	7
Mangroves (n = 28)	86	0	0	14
Freshwater swamp forest (n = 40)	79	3	10	9

Table A2: LiDAR metrics used for creating the LiDAR-Carbon models to predict ACD for the different ecosystem types.

	Code	LiDAR Metric
1	avg	Average
2	cov	Canopy cover
3	d2_10	Relative height density 0-10
4	d10_20	Relative height density 10-20
5	d20_30	Relative height density 20-30
6	dns	Canopy density
7	kur	Kurtosis
8	max	Maximum
9	min	Minimum
10	p01	Height percentile 1%
11	p05	Height percentile 5%
12	p10	Height percentile 10%
13	p25	Height percentile 25%
14	p50	Height percentile 50%
15	p75	Height percentile 75%
16	p90	Height percentile 90%
17	p95	Height percentile 95%
18	p99	Height percentile 99%
19	qav	Average square height
20	ske	Skewness
21	std	Standard deviation

Table A3: Tukey's (post-hoc) test was applied on field-measured ACD and predicted ACD. Significant difference was determined using 95% confidence intervals (Fig A5). The values stated in the table correspond to the difference between each ACD dataset and the mean of all ACD dataset for each forest ecosystem type and year.

ACD comparisons (Mg C ha^{-1})	2019			2014		
	Differences (*p adj <0.05)			Differences (*p adj <0.05)		
	Terrestrial Forest	Freshwater swamp forest	Mangrove	Terrestrial Forest	Freshwater swamp forest	Mangrove
LiDAR-predicted and Field-measured	33.95*	29.16	-0.54	65.65*	41.19	3.96
Satellite-predicted and Field-measured	-5.17	-0.40	-14.82	-6.33	7.50	-10.44
Satellite-predicted and LiDAR-predicted model	-39.11*	-29.56	-14.28	-71.98*	-33.68	-14.40

Table A4: Mean and standard deviation (SD) of field-measured and predicted ACD for the study sites in 2019 and 2014 by forest ecosystem type. The number of samples (n) refers to the number of study sites in each forest ecosystem type.

	Forest ecosystem types	Field-measured ACD ± SD (Mg C ha^{-1})	LiDAR-predicted ACD ± SD (Mg C ha^{-1})	Satellite-predicted ACD ± SD (Mg C ha^{-1})
2019				
1	Terrestrial Forest (Primary and Secondary) (n = 196)	116.87 ± 91.29	150.82 ± 51.11	111.70 ± 12.28
2	Freshwater swamp forest (n = 24)	120.30 ± 97.61	149.46 ± 47.02	119.90 ± 22.39
3	Mangrove (n = 51)	108.88 ± 63.51	108.34 ± 30.33	94.06 ± 18.06
2014				
1	Terrestrial Forest (Primary and Secondary) (n = 216)	113.34 ± 106.57	178.99 ± 92.49	107.01 ± 39.70
2	Freshwater swamp forest (n = 21)	120.20 ± 109.76	161.40 ± 45.90	127.70 ± 17.25
3	Mangrove (n = 40)	118.12 ± 74.58	122.08 ± 11.68	107.68 ± 10.54

https://www.nus.edu.sg/cncs/

NUSCNCS

Natureforclimate

NUSCNCS

NUS CNCS

NUS Centre for Nature-based Climate Solutions